LEAFY interacts with WHEAT ORTHOLOG OF APO1 to regulate spikelet number per spike in wheat

Francine Paraiso[1,2*], Junli Zhang[1*], Huiqiong Lin[1,2*], Chengxia Li[1,2], Daniel P. Woods[1,2], Tianyu Lan[3], Juan M. Debernardi[1], Anna Joe[1,2], Jorge Dubcovsky[1,2#]

[1] Department of Plant Sciences, University of California, Davis, CA 95616, USA.

[2] Howard Hughes Medical Institute, Chevy Chase, MD 20815, USA.

[3] Institute for Plant Genetics, Heinrich Heine University, Düsseldorf 40225, Germany

* The first three authors contributed equally to this work

Corresponding Author

Jorge Dubcovsky. E-mail: jdubcovsky@ucdavis.edu, Phone: +1-530-752-5159

Keywords: LEAFY, WAPO1, wheat, spike development, spikelet number, single-molecule fluorescence in-situ hybridization (smFISH)

Running Title: *LFY* regulates spike development

Summary Statement

In this study, we demonstrate that physical and genetic interactions between LFY and WAPO1 are critical to regulate spikelet number per spike, and we identify an optimum allele combination for wheat improvement.

Abstract

In wheat, the transition of the inflorescence meristem (IM) to a terminal spikelet determines the spikelet number per spike (SNS) and the maximum number of grains. In this study, we demonstrate that the plant-specific transcription factor LEAFY (LFY) physically interacts with WHEAT ORTHOLOG OF APO1 (WAPO1), a protein encoded by a gene underlying a major QTL for SNS in wheat. Loss-of-function mutations in *LFY, WAPO1*, or both result in significant and similar reductions in SNS, which indicates that both genes are required to maintain IM indeterminacy and prevent a precocious transition to a terminal spikelet. We also identify a significant genetic interaction between *LFY* and *VERNALIZATION1* (*VRN1*) and show that these genes play opposite roles in the regulation of SNS. To understand these interactions, we characterized the spatio-temporal distribution of these and other flowering genes during wheat spike development using single-molecule fluorescence *in-situ* hybridization. Finally, we identify natural *LFY-B* alleles that affect SNS, determine their interactions with natural alleles of *WAPO-A1*, and select an allele combination that maximizes SNS for wheat improvement.

Introduction

Every year, trillions of wheat spikes mature worldwide carrying the grains that provide one-fifth of the calories and proteins consumed by the human population (FAOSTAT, 2017). Therefore, increasing the maximum number of grains that can be carried by each spike can contribute to the urgent need to increase wheat productivity to feed a growing human population.

Wheat spikes, as other grass inflorescences, are comprised of specialized organs called spikelets, which are short indeterminate branches. Each spikelet has two proximal sterile bracts (glumes) followed by a variable number of florets, each subtended by a bract (lemma) with an axillary flower (Preston *et al.*, 2009, Debernardi *et al.*, 2020a). The wheat inflorescence meristem (IM) produces multiple lateral spikelet meristems (SM) in a distichous order before transitioning to a terminal spikelet. This transition determines the spikelet number per spike (SNS) and limits the maximum number of grains that can be formed in the spike. Therefore, the regulation of the timing of the transition between the IM and the terminal spikelet (henceforth, IM>TS) is critical for the determination of the maximum potential number of grains per spike.

The timing of the IM>TS transition in wheat is affected by multiple environmental conditions including drought, salt stress, heat and reduced nutrients, all of which result in reduced SNS (Frank and Bauer, 1982, Frank *et al.*, 1987, Maas and Grieve, 1990). However, differences in SNS also have a strong genetic component, with broad sense heritability for this trait ranging from $H^2 = 0.84$ in irrigated fields to $H^2 = 0.59$ in water stressed environments (Zhang *et al.*, 2018). This high heritability has facilitated the identification of several wheat genes involved in the regulation of the IM>TS transition. *VERNALIZATION1*(*VRN1*), *FRUITFULL2* (*FUL2*) and *FUL3*, the wheat homologs of Arabidopsis *SQUAMOSA* MADS-box genes *APETALA1* (*AP1*), *CAULIFLOWER* (*CAL*) and *FUL*, were found to be essential for spikelet development and for the regulation of the IM>TS transition (Li *et al.*, 2019). Loss-of-function mutations in *vrn1* or *ful2* result in normal plants with significant increases in SNS. However, in the *vrn1 ful2* mutant the IM remains indeterminate and lateral spikelets are converted into tiller-like organs with vestigial floral organs. These vestigial floral organs disappear in the *vrn1 ful2 ful3* higher order mutant, in which spikelets revert to vegetative tillers subtended by leaves (Li *et al.*, 2019).

Genes that regulate *VRN1* expression have been shown to affect SNS indirectly. *FT1*, the wheat homolog of Arabidopsis florigen *FLOWERING LOCUS T* (*FT*), binds directly to the *VRN1*

promoter as part of a floral activation complex, and functions as a transcriptional activator (Li and Dubcovsky, 2008, Li *et al.*, 2015). Mutants (or knock-down transgenic plants) of *FT1* (Lv *et al.*, 2014) or its closest paralog *FT2* (Shaw *et al.*, 2019) show reduced or delayed expression of *VRN1* and significant increases in SNS, whereas overexpression of these genes result in a precocious IM>TS transition and spikes with very few spikelets (Lv *et al.*, 2014, Shaw *et al.*, 2019). Similarly, mutations in *PPD1* that reduce or delay *FT1* expression result in SNS increases (Shaw *et al.*, 2013), whereas mutations in *ELF3* that that result in the upregulation of *FT1* and *VRN1* expression reduce SNS (Alvarez *et al.*, 2016). *bZIPC1* encodes a protein that physically interacts with FT2, and its mutants also show a large decrease in SNS (Glenn *et al.*, 2023).

However, the underpinning mechanism by which the recently cloned gene *WHEAT ORTHOLOG OF APO1* (*WAPO1*) (Kuzay *et al.*, 2019, Kuzay *et al.*, 2022) regulates SNS has not yet been elucidated. *WAPO1* is orthologous to the *Oryza sativa* (rice) gene *ABERRANT PANICLE ORGANIZATION1* (*APO1*), and to the Arabidopsis gene *UNUSUAL FLORAL ORGANS* (*UFO*), which are both involved in floral development (Levin and Meyerowitz, 1995, Ikeda *et al.*, 2007). In addition to floral defects, loss-of-function mutations in *WAPO1* or *APO1* result in significant reductions in SNS in wheat (Kuzay *et al.*, 2022) and number of panicle branches in rice (Ikeda *et al.*, 2005), respectively. These results indicate that both *WAPO1* and *APO1* promote IM indeterminacy and prevent a precocious transition of the IM into a terminal spikelet.

In Arabidopsis, UFO physically interacts with the plant-specific transcription factor LEAFY (LFY) (Lee *et al.*, 1997, Chae *et al.*, 2008, Rieu *et al.*, 2023), an interaction that is also conserved between the rice homologs APO1 and APO2 (Ikeda-Kawakatsu *et al.*, 2012). In addition, LFY activates class-A MADS-box genes *AP1* (Wagner *et al.*, 1999) and *CAL* (William *et al.*, 2004) in Arabidopsis, which are homologous to the wheat *VRN1* and *FUL2*. Since *VRN1*, *FUL2* (Li *et al.*, 2019) and *WAPO1* (Kuzay *et al.*, 2022) are all involved in the regulation of SNS, we investigated the role of *LFY* on wheat spike development.

In this study, we demonstrate that LFY physically interacts with WAPO1 in wheat protoplasts and that plants carrying loss-of-function mutations in either or both genes result in similar reductions in SNS. We also show that in wheat, *LFY* does not operate as a floral meristem identity gene as in Arabidopsis and has an opposite effect on IM determinacy. In addition, we reveal a significant genetic interaction between *LFY* and *VRN1* that modulates their opposite

effects on SNS and describe their spike spatio-temporal expression patterns using single-molecule fluorescence *in-situ* hybridization (smFISH). Finally, we characterize the effect of natural variation in *LFY* on SNS, describe its interactions with natural variants of *WAPO1*, and identify optimal allele combinations that maximize SNS.

Results

Natural variants in *LFY* affects SNS in wheat

To test if *LFY* was associated with natural variation in SNS, we explored a set of wheat Nested Association Mapping (NAM) populations previously characterized for this trait (Zhang *et al.*, 2018). We did not find QTLs for SNS associated with *LFY-A* (*TraesCS2A02G443100*), but we found one associated with marker IWB35244 closely linked to *LFY-B* (*TraesCS2B02G464200*) in the Berkut x PBW343 population. Lines carrying the Berkut allele showed significantly higher SNS than those with the PBW343 allele across three field trials (Table S1). To validate this result, we generated heterogeneous inbred families (HIFs) from two F_5 plants heterozygous for the *LFY-B* region. Sister $F_{5:2}$ lines homozygous for the Berkut allele showed 1.6 to 1.8 more spikelets per spike than those homozygous for the PBW343 allele ($P < 0.001$, Fig. 1A, Table S2), confirming the significant effect of this chromosome region on spike development.

To characterize wheat natural variation in *LFY-B*, we performed a haplotype analysis for an 813 kb region of chromosome arm 2BL including *LFY-B* (see Materials and Methods). The 146 SNPs identified in this region defined five haplotypes designated as H1 to H5 (Table S3). We then determined the haplotypes present in the sequenced wheat genomes (Walkowiak *et al.*, 2020), and used them to obtain the *LFY-B* sequences associated with each haplotype (Table S4). The H3 haplotype was not present among the sequenced wheat genomes, so we sequenced *LFY-B* from hexaploid wheat cultivar RAC875 and deposited the sequence in GenBank (OR753911).

Comparison of the *LFY-B* sequences associated with the different haplotypes revealed a proline to leucine change at position 34 (P34L), an arginine to serine change at position 80 (R80S), a proline deletion in a stretch of eight prolines in positions 26 to 33 (henceforth 8P to 7P), and a 220-bp insertion 872 to 653 bp upstream from the start codon (henceforth P+ and P- for the presence and absence of the insertion, respectively). The *LFY-B* allele associated with the H3 haplotype showed the combination P-,34P,80R,8P (Fig. 1B) observed in other grass species (Fig.

S1), which suggests that this is likely the ancestral combination. The *LFY-B* alleles associated with the H1 and H2 haplotypes differ from H3 by the presence of the 34L polymorphism (P-,34L,80R,8P). The 34L polymorphism was also present in the *LFY-B* alleles associated with the H4 and H5 haplotypes, but in H4 it was combined with the proline deletion (P-,34L,80R,7P) and in H5 with the 80S polymorphism and the promoter insertion (P+,34L,80S,8P) (Fig. 1B). This promoter insertion was associated with a 17 % decrease in *LFY* expression in the developing spike at the lemma primordia stage (*P*= 0.036, Fig. 1C, Table S2).

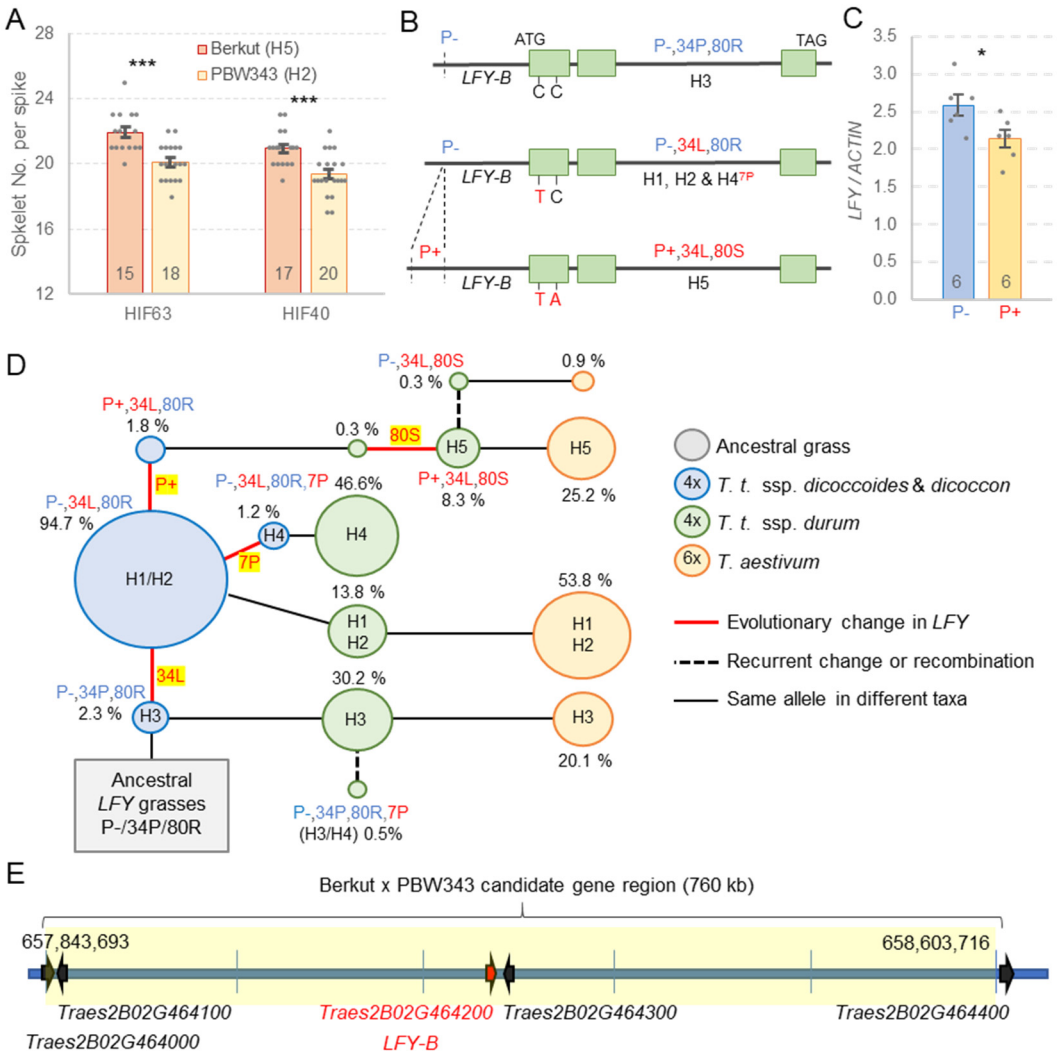

Fig. 1. Natural variation in *LFY-B* in wheat. (A) Differences in SNS between sister lines homozygous for the *LFY-B* alleles from PBW343 and Berkut in $F_{5:2}$ heterogeneous inbred families (HIFs). (B) *LFY-B* alleles differ in a promoter insertion (P+), amino acid changes P34L and R80S and a proline deletion (8P to 7P, only in H4). Derived alleles are indicated in red. (C) qRT-PCR comparison of *LFY* expression between HIF sister lines homozygous for the presence (P+) or absence (P-) of the 220-bp promoter insertion in developing spikes at the lemma primordia stage. For A and C, the number of biological replications is indicated at the base of the bars. Error bars indicate

SEM and probability values are from two tailed *t*-tests. * = $P < 0.05$, *** = $P < 0.001$. Raw data and statistics for (A) and (C) are available in Table S2. (D) Changes in *LFY-B* allele frequencies in ancestral tetraploid (blue circles), modern tetraploid (green circles) and modern hexaploid (orange circles) wheat accessions. The likely origins of the different polymorphisms are marked in red bold lines and highlighted. (E) High-density map of the *LFY-B* region based on recombination events described in Table S7.

To estimate the frequency of the different *LFY-B* alleles, we designed markers for the promoter insertion, the two non-synonymous changes (P34L and R80S) and the proline deletion (primers in Table S5), and used them to characterize 171 wild and 618 cultivated wheat accessions (Table S6). The ancestral *LFY-B* allele P-,34P,80R (H3) was found in 30.2% of the *T. turgidum* ssp. *durum* and 20.1 % of the *T. aestivum* accessions but, surprisingly, in only 2.3 % of the ancestral tetraploid species *T. turgidum* ssp. *dicoccoides* and *T. turgidum* ssp. *dicoccon* (Fig. 1D and Table S6). The derived *LFY-B* allele P-,34L,80R was the most abundant in all wheat taxa (Fig. 1D), suggesting that the 34L change was an early event in wheat evolution that was favored by selection. We did not find the R80S polymorphism among the ancestral tetraploid accessions, but found it in 8.3% of the modern durum and in 25.2 % of the common wheat varieties, which suggests positive selection in modern hexaploid wheat breeding programs. The promoter insertion was frequently associated with the 80S polymorphism in both durum (97.0 %) and common wheat (96.7 %), but was also found in combination with other alleles at very low frequencies (Fig. 1D), suggesting either recurrent changes or recombination among *LFY* alleles. Finally, we detected the 8P to 7P deletion associated with the H4 haplotype in few ancestral tetraploids (1.2 %), at a higher frequency in modern durum (46.6 %) accessions, and absent in hexaploid wheat (Fig. 1D).

We then generated a high-density map to confirm the linkage between the SNS QTL and the *LFY-B* polymorphisms in the Berkut (H5) x PBW343 (H2) HIF population. To identify recombination events in the region, we screened 770 segregating chromosomes with markers flanking a 3 Mb region encompassing *LFY-B*, identified lines with recombination events, and genotyped these lines with six new markers (primers in Table S5) to identify the recombination events closest to *LFY-B* (Table S7). Progeny tests from the three lines with the closest recombination events showed significant differences in SNS between sister lines (Table S7), indicating that *LFY-B* and the QTL for SNS were linked within a 760 kb region (Table S7).

The candidate gene region includes only two complete and two partial high-confidence annotated genes in addition to *LFY-B* (Fig. 1E, Table S8). Among these genes, *TraesCS2B02G464000* and *TraesCS2B02G464100* encode proteins with kinase domains that are expressed at very low levels during spike development (VanGessel *et al.*, 2022). *TraesCS2B02G464300* is highly expressed in the developing spike (VanGessel *et al.*, 2022), but encodes a 50S ribosomal protein L11 that has no amino acid polymorphisms between the parental lines. Finally, only the promoter region of *TraesCS2B02G464400* is located within the candidate gene region, and it does not show major polymorphisms. Taken together, these results suggest that *LFY-B* is the most likely causal gene for the SNS QTL detected in the Berkut x PBW343 population. This hypothesis is supported by the significant effect of loss-of-function mutations in *LFY* described below.

Induced loss-of-function mutations in *LFY* reduce SNS and alter floret morphology

Using our sequenced Kronos mutant population (Krasileva *et al.*, 2017), we selected truncation mutations K2613 for *LFY-A* (henceforth *lfy-A*) and K350 for *LFY-B* (henceforth *lfy-B*). The *lfy-A* mutant has a G>A change in the acceptor splice site of the second intron, which results in the mis-splicing of the third exon, a shift in the reading frame, and a premature stop codon (Fig. 2A). The *lfy-B* mutant has a premature stop codon at position 249 (Q249*) that truncates 37 % of the protein (Fig. 2A). Primers used to track these mutations are described in Table S5. The mutants were backcrossed to Kronos to reduce background mutations, and intercrossed with each other to select sister lines homozygous for the different mutation combinations, including the wildtype (WT), *lfy-A*, *lfy-B*, and the *lfy-A lfy-B* combined mutant (henceforth, *lfy*).

Comparisons between the homozygous sister lines in a growth chamber, revealed a highly significant decrease (37%, $P < 0.001$) in SNS in the combined *lfy* mutant relative to the wildtype (WT, Fig. 2B-C, Table S9), and smaller but still significant decreases in the single *lfy-A* (12%) and *lfy-B* (8%) mutants (Fig. S2, Table S10). No significant differences in heading time or leaf number were detected between *lfy* and the WT (Fig. 2D-E, Table S9), suggesting a limited effect of *LFY* on the timing of the transition between the vegetative and reproductive meristems. Based on its effect on SNS, we infer that *LFY* delays the IM>TS transition.

In addition to its effects on SNS, the *lfy* mutant also showed severe alterations in floral organs. These alterations included missing or altered lodicules, mosaic lodicule-stamen organs, reduced number of stamens, and increased number of carpels. Thirteen out of the 14 flowers checked

showed one stamen and three carpels suggesting homeotic conversions of stamens to carpels (Fig. 2F). The frequent floral abnormalities, combined with the reduced SNS, resulted in low spike fertility.

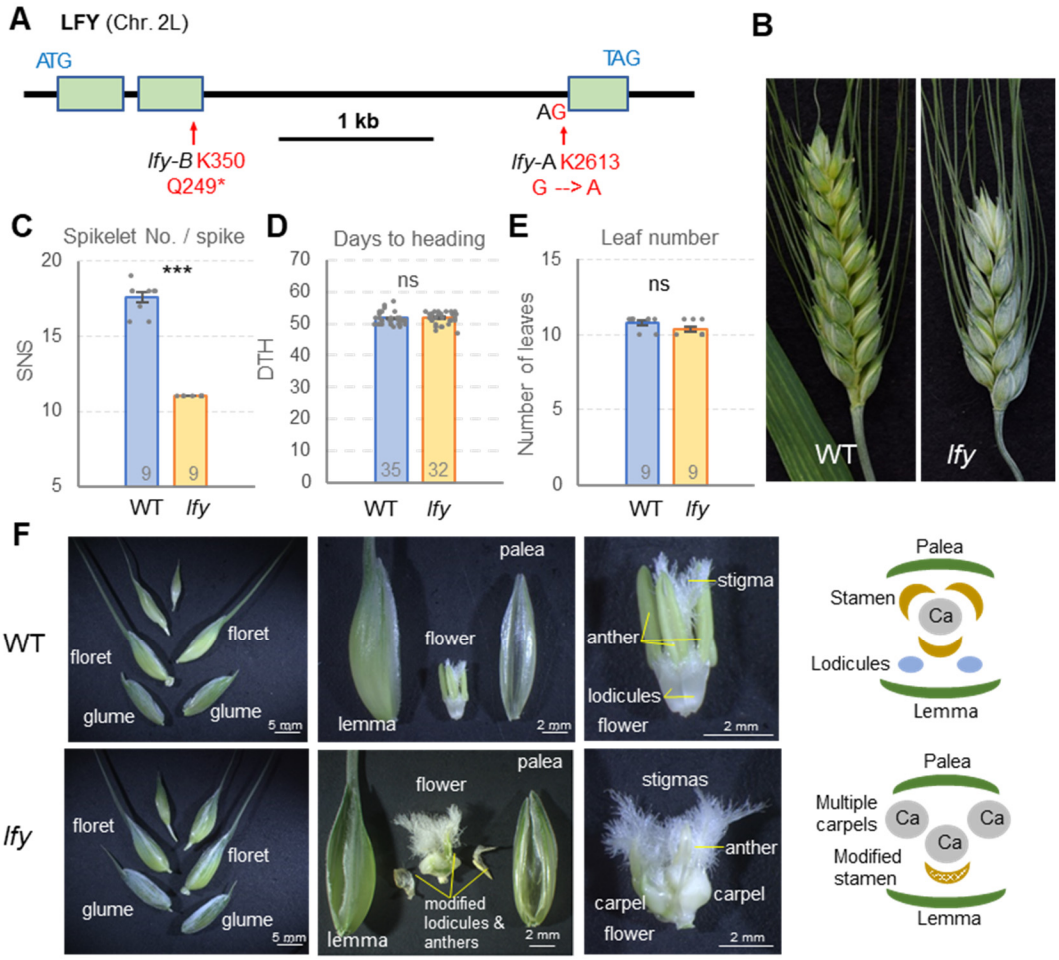

Fig. 2. *LFY* loss-of-function mutants. (A) *LFY* gene structure and location of the selected mutations in *lfy-A* and *lfy-B*. (B) Representative wildtype (WT) and *lfy* combined mutant. Comparison between WT and *lfy* for (C) spikelet number per spike, (D) days to heading, and (E) leaf number. Numbers inside the bars indicate number of biological replicates (separate plants). Raw data and statistics for C-E are available in Table S9. (F) Floral defects observed in the *lfy* mutant. A schema of the most frequent changes is presented on the right.

Overexpression of *LFY* partially rescues the reduced SNS phenotype of *lfy*

To test if *LFY* function was sufficient to rescue the mutant phenotype, we generated transgenic plants expressing the *LFY-A1* coding region driven by the constitutive maize *UBIQUITIN*, either without a tag or fused to a C-terminal HA tag. Transgenic lines for five independent *UBI:LFY* events and five independent *UBI:LFY-HA* events, all showed significantly higher *LFY* transcript

levels in the leaves than non-transgenic sister lines and wildtype Kronos, where expression of endogenous *LFY* was not detected (Fig. S3, Table S11).

We then crossed both the *UBI:LFY* and *UBI:LFY-HA* transgenic plants with the *lfy* mutant and in the progeny, selected sister lines homozygous for *lfy* mutations or for wildtype alleles (WT), each with or without the transgenes. Among the plants without the transgene, the *lfy* allele was associated with a significant reduction in the number of spikelets per spike (6.6 spikelets, $P < 0.001$), as in previous experiments. No significant differences in SNS were observed between *UBI:LFY* and *UBI:LFY-HA* plants so data was combined for statistical analyses. In the presence of the wildtype *LFY* alleles, transgenic plants showed 1.1 more spikelets per spike than non-transgenic control ($P = 0.0045$, Fig. 3, Table S12), whereas in the *lfy* mutant, the transgenic lines showed a highly significant increase in SNS (4 spikelets increase, $P < 0.001$, Fig. 3). Within the *lfy* mutants, plants carrying the transgene showed improved fertility (Table S12). These results demonstrate that constitutive expression of *LFY* can partially complement the effect of the *lfy* mutant on SNS and fertility.

Taken together, the results from the high-density genetic mapping and the effects of the *lfy* mutants and transgenic plants, all indicate that *LFY* is the causal gene of the 2BL QTL for SNS detected in the Berkut x PBW343 segregating population.

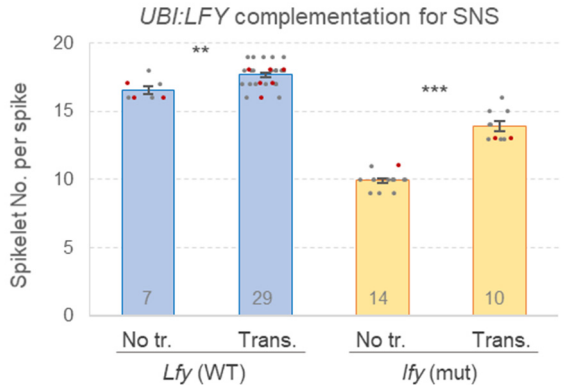

Fig. 3. **Effect of *UBI:LFY* and *UBI:LFY-HA* on spikelet number per spike (SNS).** No significant differences were detected between *UBI:LFY* (grey dots) and *UBI:LFY-HA* (red dots) so data were analyzed together. The effect of the transgenes on SNS was evaluated in both the wildtype (WT) and *lfy* mutant backgrounds. Numbers within the bars indicate the number of independent biological replicates. *P* values correspond to two-tail *t*-tests between transgenic and non-transgenic (No tr.) lines in the same *LFY* background. ns = not significant, ** = $P < 0.01$, and *** = $P < 0.001$. Raw data is available in Table S12.

LFY interacts with WAPO1 in wheat leaf protoplasts

Since *LFY* and *WAPO1* mutants were both associated with similar reductions in SNS (Kuzay *et al.*, 2022), and their homologous proteins interact with each other in Arabidopsis (Chae *et al.*, 2008), we tested the ability of LFY and WAPO1 to interact physically with each other in wheat. We tested the interaction between LFY-A and the two WAPO-A1 natural alleles, which differ in the presence of a cysteine or a phenylalanine at position 47 within the F-box domain (47F is associated with higher SNS than C47) (Kuzay *et al.*, 2022). We co-transformed wheat leaf protoplasts with *UBI:LFY-HA* combined with either *UBI:WAPO1-47C-MYC* or *UBI:WAPO1-47F-MYC*. After immunoprecipitation with anti-MYC beads, we detected LFY-HA using an anti-HA antibody in both the WAPO1-47C-MYC and WAPO1-47F-MYC precipitates (Fig. 4). Thus, LFY can interact with either WAPO1 variant.

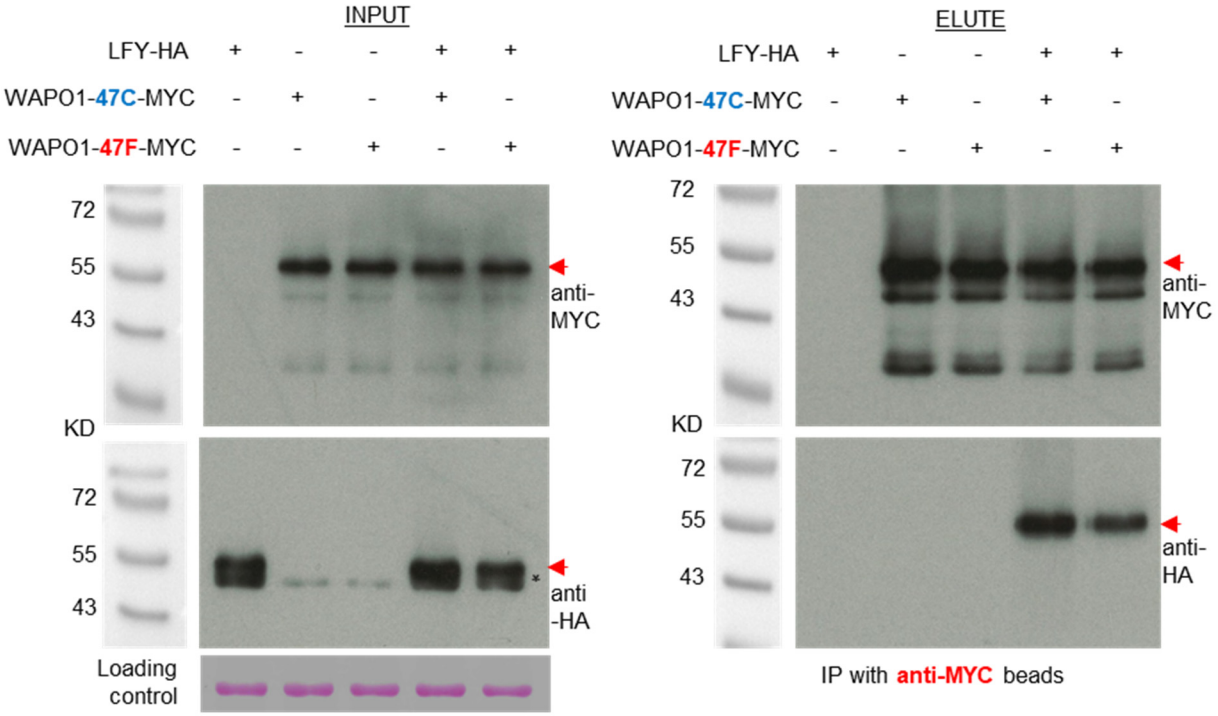

Fig. 4. **Physical interaction between WAPO1 and LFY proteins.** The interaction between LFY and both WAPO1 alleles (47F and 47C) was tested in tetraploid wheat leaf protoplasts by co-immunoprecipitation (coIP). (Left) Input and loading control. (Right) Elute showing LFY-HA signal using an anti-HA antibody in both the WAPO1-47C-MYC and WAPO1-47F-MYC precipitates with anti-MYC beads.

LFY and *WAPO1* show dynamic expression profiles during wheat spike development

For the LFY-WAPO1 interaction described above to be biologically relevant, the spatial and temporal expression of the two proteins needs to have some overlap. A previous RNA-seq study including different tissues at different developmental stages in CS, detected *LFY* and *WAPO1* transcripts in developing spikes and elongating stems (Choulet *et al.*, 2014). A separate RNA-seq study including five spike developmental stages in tetraploid wheat Kronos (VanGessel *et al.*, 2022), showed transcripts for both genes present at the different stages. *LFY* transcript levels were more abundant than those of *WAPO1*, and both genes showed lower transcript levels at the vegetative stage than at the double-ridge to floret primordia stages (Fig. S4, Table S13). These studies indicate that *LFY* and *WAPO1* are present at the same times during spike development.

To refine the position of *LFY* and *WAPO1* transcripts within the developing spike, we examined their dynamic spatial patterns using smFISH (Fig. 5). During the transition between the vegetative and reproductive phases (W1.5), *LFY* transcripts were concentrated in bands radiating from the axis of the elongating shoot apical meristem (SAM) towards the lateral primordia (Fig. 5A). *LFY* transcripts were not abundant at the tip of the IM at this or later developmental stages (Fig. 5C-D). At the late double-ridge stage (W2.5), in the less developed lateral meristems present at the bottom (Fig. 5B) and top (Fig. 5C) of the developing spike, *LFY* expression was stronger at the leaf ridge (also known as lower ridge) than at the spikelet or upper ridge (blue arrows). A spatial differentiation was also evident in the more mature spikelet meristems (SMs), where *LFY* expression was abundant except for the central-distal regions (Fig. 5B, blue arrows). Some SMs showed a more uniform distribution of *LFY*, but we think those can be the result of off-centered sections. At the lemma primordia stage (W3.25), close to the formation of the terminal spikelet, *LFY* expression in the distal region of the spike (IM or IM plus first two SMs) was significantly lower (78-80%) than at the late double ridge stage (Fig. 5D, Table S14).

In the more mature spikelets located at the center of the developing spike, *LFY* also showed a non-uniform distribution. Distal to the lemma primordia, *LFY* was highly expressed within a narrow region (similar to a bird's nest) that delimited a distal region of low *LFY* expression. These distal regions of low *LFY* expression largely overlap with the areas where *WAPO1* is expressed in the spikelets (Fig. 5D, white arrows).

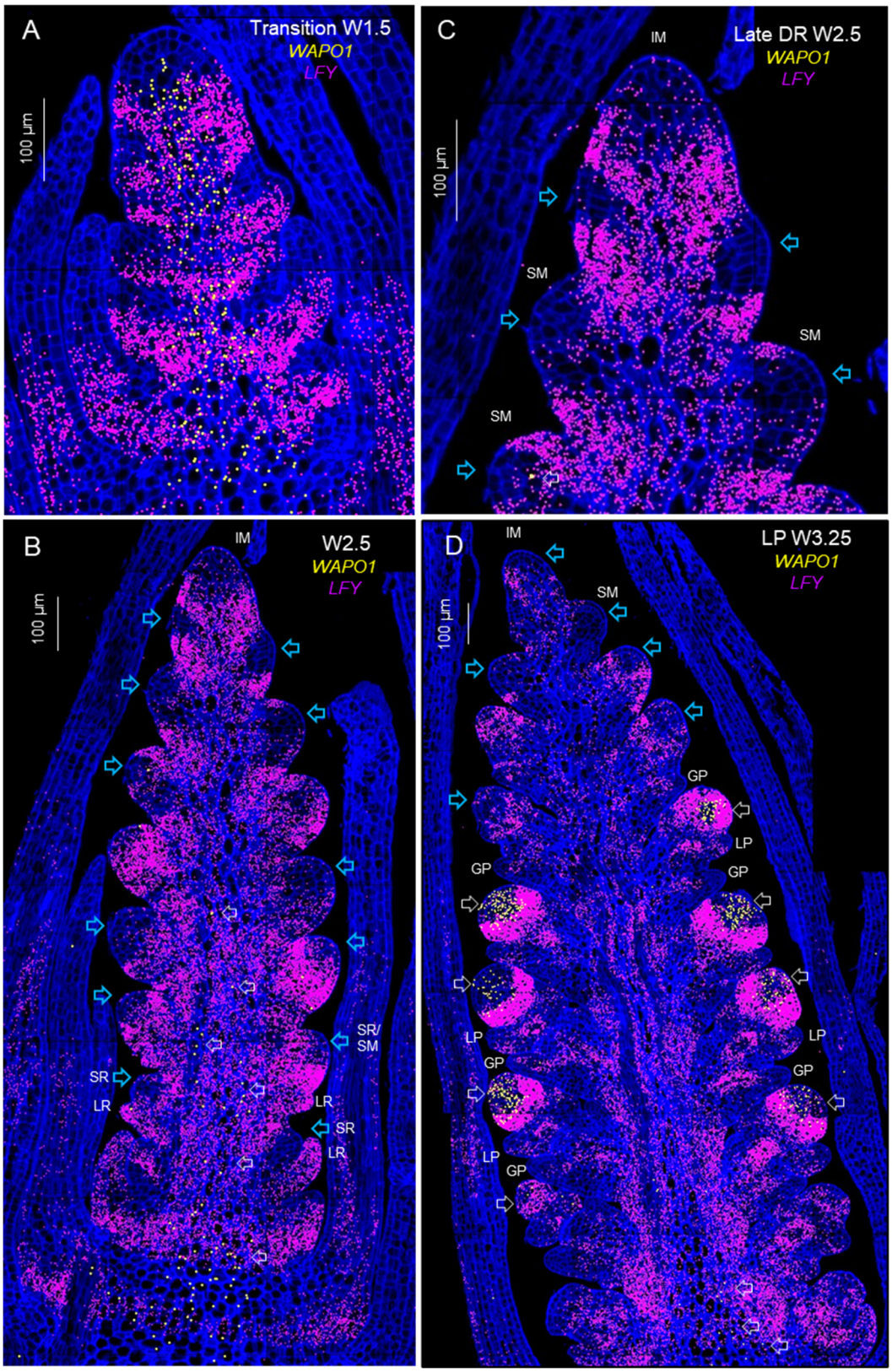

Fig. 5. **Single-molecule fluorescence in-situ hybridization (smFISH) of *LFY* and *WAPO1* during wheat spike development.** Cell walls stained with calcofluor are presented in dark blue. Additional figures without *LFY* are

available in Fig. S5 to facilitate *WAPO1* visualization. (A) Elongated shoot apical meristem transitioning to an inflorescence meristem (IM, W1.5). (B) Late double ridge stage (W2.5). (C) Detail of the IM region from (B). (D) Lemma primordia stage (W3.25). In B and D, *WAPO1* (yellow dots, white arrows) was detected at the central region at the base of the spike. Blue arrows indicate regions of the spikelet meristems (SMs) where *LFY* (pink dots) is excluded or expressed at lower levels. The spike in D has 18 lateral SM so it is close to the IM>TS transition. LR = leaf ridge, SR = spikelet ridge, GP = glume primordium, LP = lemma primordium. Scale bars are 100 µm.

WAPO1 transcripts were detected from the early W1.5 at the axis of the developing spike (Fig. 5A and S5), in a region that overlapped with *LFY*. At later stages (W2.5 and W3.25), however, *WAPO1* expression was restricted to the base and center of the developing spike, likely in differentiating vascular tissue (Fig. 5B and D). To facilitate the visualization of the less abundant *WAPO1* transcripts, additional images are presented at Fig. S5 including only *WAPO1* transcripts. At the lemma primordia stage (W3.25), *WAPO1* was also expressed at the distal part of the more developed spikelets, in the region where *LFY* transcripts were low (Fig. 5D and S5C-D). In summary, the complementary expression domains of *LFY* and *WAPO1* in the developing spikelets generate an overlapping contact area, which we hypothesize favors their protein interactions and provides important spatial information for normal floral development.

Spatio-temporal expression profiles of meristem and floral organ identity genes

To understand the relationship between *LFY* and *WAPO1* expression domains and those of other floral genes, we explored the spatial distribution of several MADS-box genes including the class-A meristem identity genes *VRN1* and *FUL2* (Li *et al.*, 2019), and the class-B, class-C and class-E floral organ identity genes (Table S15). The latter were previously shown to be regulated by *LFY* and *WAPO1* in barley and wheat, respectively (Selva *et al.*, 2021, Kuzay *et al.*, 2022), so we first tested if *VRN1* and *FUL2* transcript levels were also regulated by *LFY* using qRT-PCR (Fig. S6, Table S16). We found no significant differences between *lfy* and the wildtype control for *VRN1* or *FUL2* transcript levels at W2.0 and W3.0 (Fig. S6).

We then compared the expression profiles of these genes using smFISH. At the late vegetative stage (W1.0), *VRN1* and *LFY* were expressed at low levels, and *FUL2* was not detected (Fig. 6A). During the transition to the reproductive stage (W1.5), a few *FUL2* transcripts were detected (orange arrows) and both *LFY* and *VRN1* transcript levels increased, with *VRN1* showing a more uniform distribution than *LFY* (Fig. 6B).

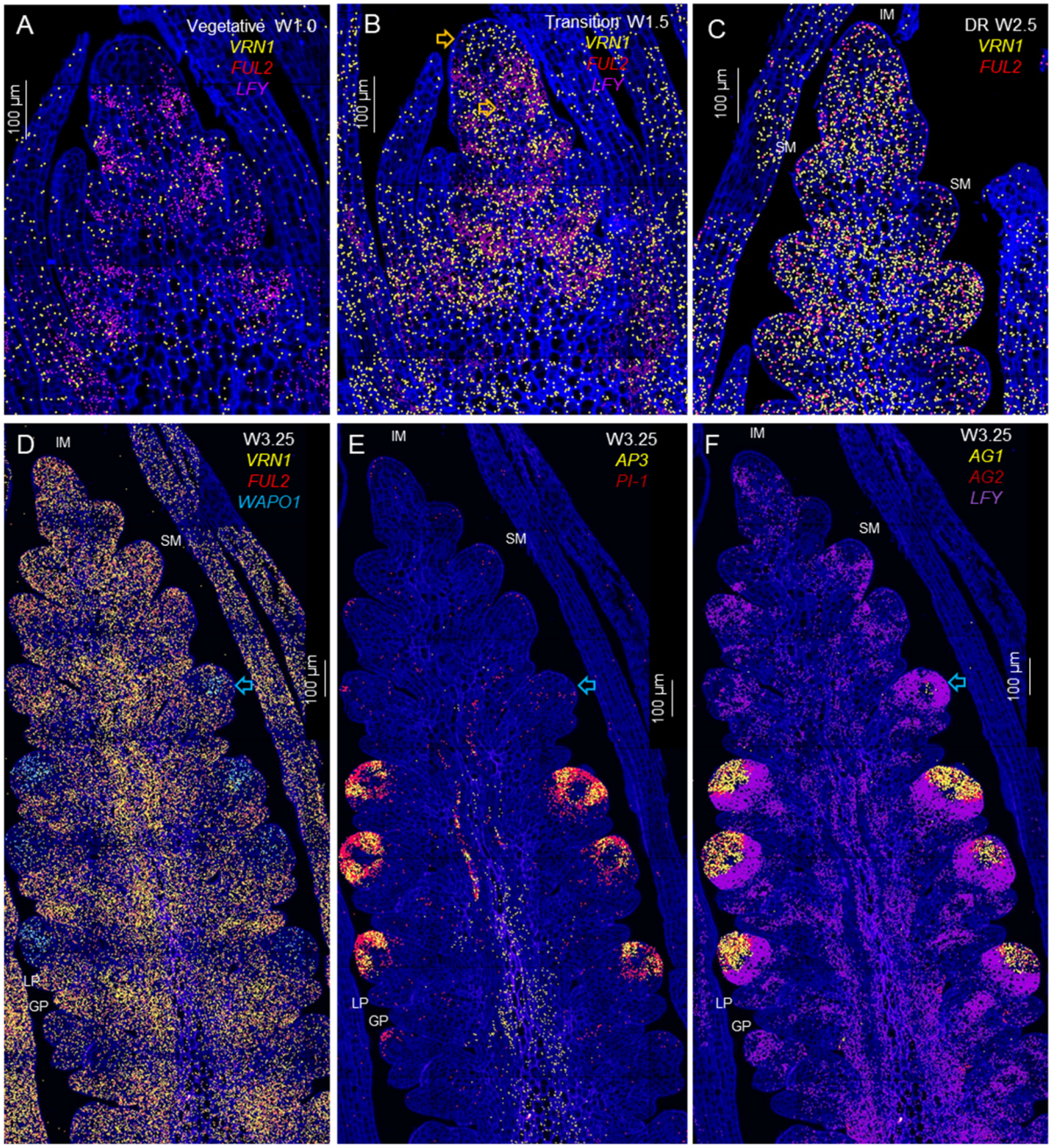

Fig. 6. **Transcription profiles of *LFY*, *WAPO1* and MADS-Box floral genes during wheat spike development.** Cell walls stained with calcofluor are presented in dark blue. (A-B) Relative distribution of *VRN1* (yellow), *FUL2* (red) and *LFY* (violet). (A) Late vegetative SAM W1.0 (no *FUL2*). (B) Transitioning SAM W1.5 (limited *FUL2*, orange arrows). (C) *VRN1* and *FUL2* at the late double ridge stage (W2.5) (D-F) Lemma primordia stage (W3.25). (D) *VRN1* (yellow), *FUL2* (red) and *WAPO1* (light blue). (E) Class-B MADS-box genes *AP3* (yellow) and PI-1 (red). (F) Class-C MADS-box genes *AG1* (yellow) and *AG2* (red) relative to *LFY* (violet). The blue arrow indicates a young spikelet where *WAPO1* is expressed earlier than the class-B and class-C MADS-box genes. IM =

inflorescence meristem, SM = spikelet meristem, GP = glume primordium, LP = Lemma primordium. Gene identifications based on CS RefSeq v1.1 and rice orthologs are provided in Table S15.

At the later stages (W2.5 and W3.25) both *VRN1* and *FUL2* were highly and uniformly expressed in the IM and young SMs (Fig. 6C-D). However, in the most mature spikelets, *VRN1* and *FUL2* expression was stronger at the glume and lemma primordia than in the distal region that overlapped with *WAPO1* expression (Fig. 6D). *FUL3*, showed a similar expression profile as *FUL2*, but it is presented separately because of its lower expression levels (Fig. S7) and more limited impact on SNS (Li *et al.*, 2019).

In the more mature spikelets (with glume and lemma primordia) at the center of the developing spike, the transcripts of the class-B (*AP3* and *PI-1*, Fig. 6E), class-C (*AG1*and *AG2*, Fig. 6F) and class-E (*SEP3-1* and *SEP3-2*, Fig. S8) floral organ identity genes were concentrated in the region distal to the high *LFY* expression, which overlapped with the *WAPO1* expression domain (Fig. 6D). *WAPO1* was detected in younger spikelets than the floral organ identity genes (Fig. 6D-F blue arrow), suggesting an earlier upregulation of *WAOP1* relative to the other floral genes. *SEP1-2*, *SEP1-4*, and *SEP1-6* were expressed outside of the previous region (Fig. S8), suggesting functional divergence with the *SEP3* genes.

In summary, the high expression level of the floral organ identity genes within the spikelet region overlapping with *WAPO1* expression and *LFY* reduced expression, suggests that these two genes may contribute to the delimitation of the expression domains of the floral organ identity genes and to the floral defects observed in the *wapo1* and *lfy* mutants.

***LFY* and *WAPO1* show significant genetic interactions for SNS**

To test if the physical interaction between LFY and WAPO1 was reflected in a genetic interaction for SNS, we intercrossed the *lfy* and *wapo1* mutants. Due to the highly reduced fertility of the homozygous *lfy* mutants (Table S12), we first selected lines homozygous for the *lfy-A* mutant allele and heterozygous for *lfy-B* among F_2 and F_3 progenies. We then screened a large F_4 segregating population and selected the four homozygous classes (WT, *lfy*, *wapo1*, and combined *lfy wapo1*) using molecular markers (primers in Table S5). Plants homozygous for mutations in both *LFY* (*lfy*) or in both *WAPO1* (*wapo1*) homeologs showed large and similar reductions in SNS relative to the wildtype (34% and 35% reduction, respectively, Fig. 7A).

Interestingly, the combined *lfy wapo1* mutant showed a reduction of 38%, which was not significantly different from the reductions observed in the single mutants (Fig. 7A, Table S17). These results suggest that both LFY and WAPO1 proteins are required to suppress a precocious IM>TS transition.

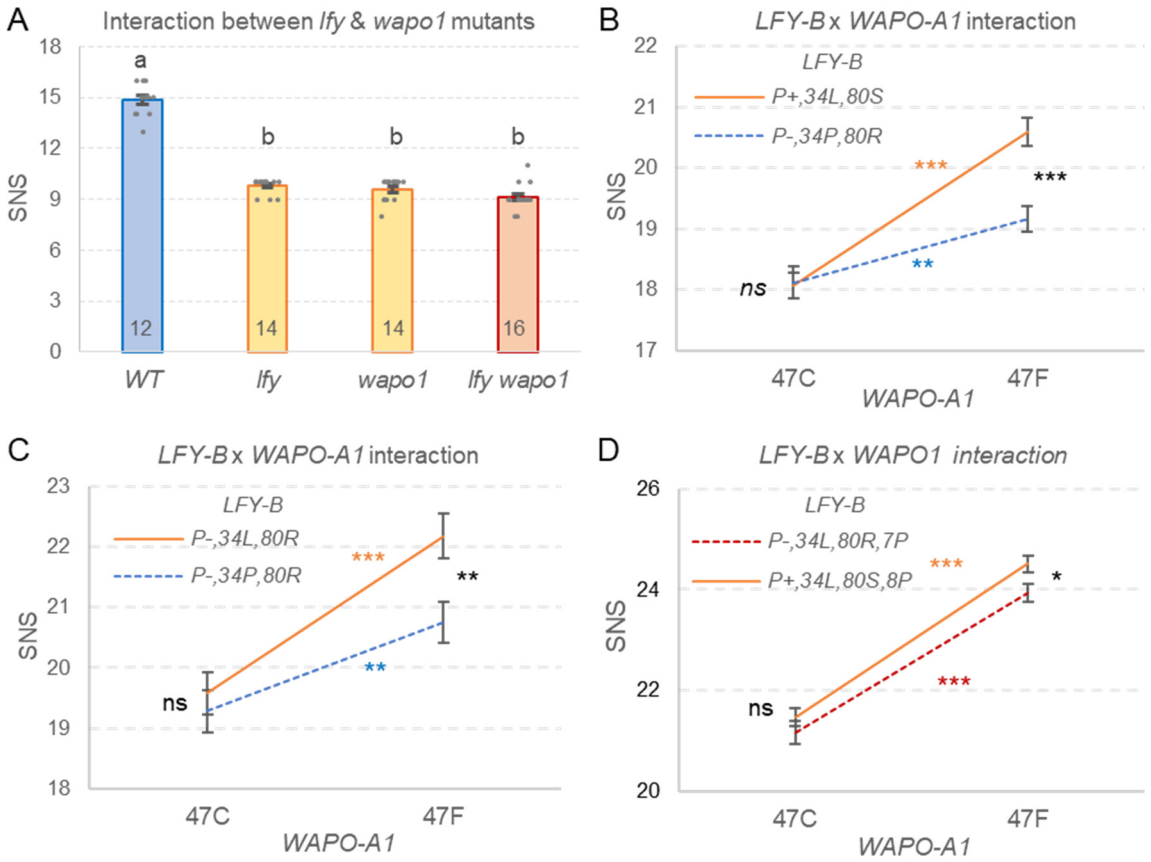

Fig. 7. Epistatic interactions for SNS between *LFY* and *WAPO1*. (A) Interaction between loss-of-function *lfy* and *wapo1* mutants. Different letters above the bars indicate significant differences in Tukey tests ($P < 0.05$), and numbers inside the bars the number of biological replications (B-D) Interactions between *WAPO-A1* and *LFY-B* natural alleles. (B) Berkut x RAC875 RILs evaluated in 6 environments, total N = 390 (Zhang *et al.*, 2018). (C) RSI5 x RAC875. Results from the combined ANOVA of 3 experiments using experiment as block, total N = 118. (D) Combined analysis of tetraploid populations Kronos x PI 519639 and Kronos/Gredho/Kronos-47F evaluated in the field. *P* values indicate the significance of the four possible contrasts in the ANOVAs described in Table S18. ns = not significant, * = $P < 0.05$, ** = $P < 0.01$, and *** = $P < 0.001$. Error bars are SEM. Raw data and statistics are available for (A) in Table S17 and for (B-D) in Table S18.

We then investigated the interactions between natural *LFY-B* alleles (Fig. 1B) and *WAPO-A1* alleles identified previously (47C and 47F) (Kuzay *et al.*, 2019, Kuzay *et al.*, 2022) in three

different segregating populations (Fig. 7B-D, Table S18). In the Berkut x RAC875 RIL population, which was evaluated in 6 environments (Zhang *et al.*, 2018), we observed significant effects on SNS for both *WAPO-A1* ($P < 0.001$) and *LFY-B* ($P = 0.0028$), as well as a significant interaction ($P = 0.0013$). The effect of *LFY* on SNS was significant only in the presence of the *WAPO-A1* allele 47F, and among those plants the ones carrying the *LFY-B* allele P+,34L,80S showed 1.4 more spikelets per spike than the plants with the P-,34P,80R allele ($P < 0.001$, Fig. 7B). The effect of *WAPO-A1* was significant in the presence of both *LFY-B* alleles, but was stronger in the presence of the *LFY-B* allele P+,34L,80S (2.5 spikelets/spike) than in the presence of P-,34P,80R (1.0 spikelets per spike, Fig. 7B).

The second population, RSI5 x RAC875, segregated for the *LFY-B* polymorphism L34P (both lines are P-/80R/8P) and for the *WAPO-A1* polymorphism C47F. This population showed significant effects on SNS for both *WAPO-A1* ($P < 0.001$) and *LFY-B* ($P = 0.0165$). The interaction was not statistically significant ($P = 0.1142$) but, as in the previous population, *LFY-B* showed a stronger effect on SNS in the presence of the *WAPO-A1* 47F allele (1.4 spikelets/spike, $P = 0.0056$) than the 47C allele (0.3 spikelets/spike, $P = 0.5481$, Fig. 7C).

Finally, we studied the effect of the *LFY-B* alleles P+,80S,8P and P-,80R,7P on SNS in a fixed 34L background. We combined the analyses of two tetraploid wheat populations where the durum line Kronos (H4, P-,34L,80R,7P and *WAPO-A1* 47C) was crossed with two different tetraploid lines carrying the P+,34L,80S,8P allele (H5). The *WAPO-A1* 47F allele was present in one of the parental lines and was introgressed from Kronos-47F (PI 698810) to develop the second segregating population (see Materials and Methods). The P+,80S,8P allele was associated with a significant increase in SNS ($P = 0.0205$), which was stronger in the presence of the *WAPO-A1* allele 47F (0.6 spikelets/spike, $P = 0.0190$) than in the presence of 47C, where no significant differences were detected ($P = 0.2892$, Fig. 7D). The differences between *WAPO-A1* 47F and 47C alleles were significant in the presence of both *LFY-B* alleles ($P < 0.0001$, Fig. 7D).

We speculate that the 7P polymorphism associated with P-,34L,80R may have a small positive effect on SNS, reducing the difference in SNS with the also favorable allele P+,34L,80S,8P (0.6 spikelets per spike) relative to the differences between this last allele and P-,34L,80R,8P observed in the Berkut x PBW343 population (1.7 spikelets/spike, Table S18). This hypothesis

would be consistent with the rapid increase of the frequency of the 7P polymorphism among the commercial tetraploid wheat varieties (Fig. 1D).

In summary, in all three populations the positive effects of the derived *LFY-B* alleles on SNS relative to the ancestral allele (P-,34P,80R) were significant only in the presence of the *WAPO-A1* 47F allele (high SNS).

Genetic interactions between *LFY* and class-A MADS-box genes

Class-A MADS-box genes *VRN1* and *FUL2* promote the IM>TS transition whereas *LFY* represses or delays this transition. Given the opposite effects of these genes in the IM>TS transition, we examined their epistatic interactions for SNS. We crossed a plant homozygous for *lfy-A* and heterozygous for *lfy-B* (to maintain fertility) with mutants homozygous for *vrn1* and *ful2*-A but heterozygous for *ful2*-B and, in the progeny, selected sister plants homozygous for the four gene combinations (WT, *lfy*, *vrn1*, and combined *lfy vrn1*).

A factorial ANOVA including the four homozygous gene combinations showed highly significant effects on SNS for both *VRN1* and *LFY*, and a highly significant interaction ($P < 0.0001$, Fig. 8A, Table S19). The effect of *LFY* on SNS was stronger in the *vrn1* mutant (10.3 spikelets) than in the presence of the functional *Vrn1* allele (5.2 spikelets). By contrast, the effect of *VRN1* on SNS was stronger in the presence of the functional *LFY* allele (9.1 spikelets) than in the presence of *lfy* (4.0 spikelets, Fig. 8A). *VRN1* also showed highly significant effects on the number of leaves and heading time, similar to previous studies (Li *et al.*, 2019), while *LFY* showed no-significant differences for these traits in the presence of the *Vrn1* or *vrn1* alleles. No significant interactions were detected for these two traits (Fig. 8B-C, Table S19).

The effect of *FUL2* on SNS was smaller than the effect of *VRN1* (Fig. 8D) and the interaction with *LFY* was not significant (Table S19). However, the trends were similar to those observed in the interactions between *LFY* and *VRN1*: a stronger effect of *LFY* on SNS in the presence of the mutant *ful2* allele (6.3 spikelets) than the wildtype *Ful2* allele (5.6 spikelets), and a stronger effect of *FUL2* in the presence of wildtype *LFY* allele (1.6 spikelets) than in the presence of the *lfy* mutant (0.9 spikelets).

To test if a direct interaction between LFY and the *VRN1* promoter can contribute to the genetic interaction between these genes, we performed a yeast-one-hybrid (Y1H) assay. The experiment

confirmed that LFY can bind to a 108 bp segment from the *VRN1* promoter (-328 to -221 upstream of the start codon) including a predicted LFY binding site (CCAATGG) in the Y1H assay (Fig. S9).

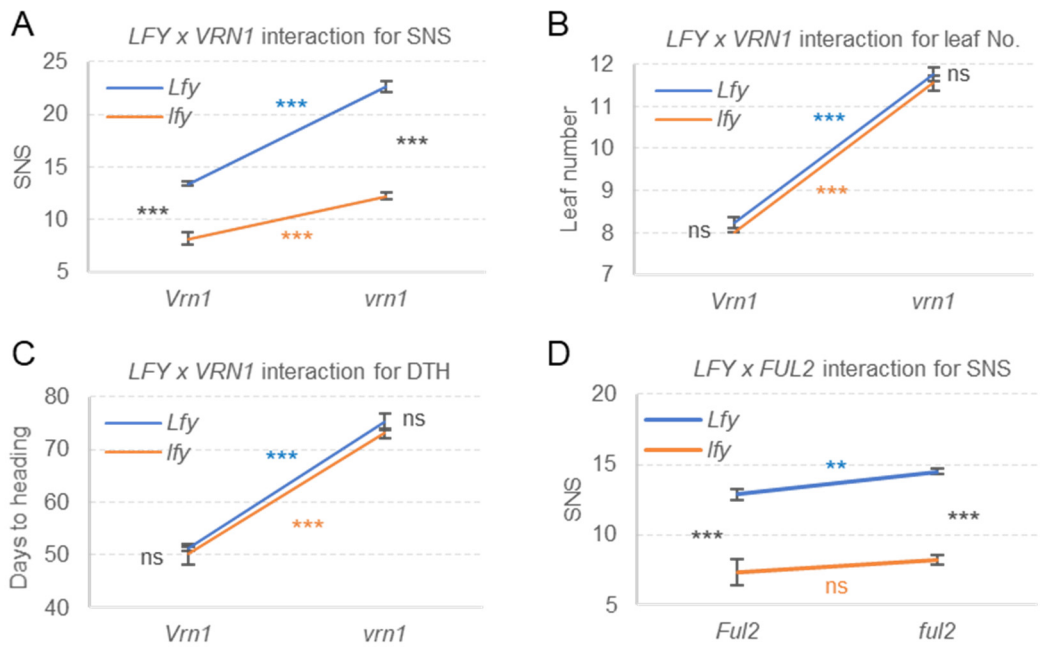

Fig. 8. Genetic interactions between *LFY* and both *VRN1* and *FUL2*. (A-C) Interactions between *LFY* and *VRN1* for (A) spikelet number per spike (SNS) (total N = 34), (B) leaf number (total N = 34), and (C) days to heading (total N = 34). (D) Interaction between *LFY* and *FUL2* for SNS (total N = 23). *P* values indicate the significance of the four possible contrasts in the ANOVAs described in Table S19. ns = not significant, * = $P < 0.05$, ** = $P < 0.01$, and *** = $P < 0.001$. Error bars are SEM. Raw data and statistics are available in Table S19.

Discussion

Similarities and differences in *LFY* function between Arabidopsis and wheat

Floral defects in the wheat *lfy* mutants are concentrated in the three inner whorls, including lodicules, stamens and carpels (Fig. 2). Similar defects have been observed in mutants for *LFY* orthologs in other grass species, including *apo2* in rice (Ikeda-Kawakatsu *et al.*, 2012), *multiovary 5* in barley (Selva *et al.*, 2021), and *zfl1 zfl2* in maize (Bomblies *et al.*, 2003). In Arabidopsis, weak *lfy* mutants also have defects concentrated in the three inner floral whorls, whereas strong *lfy* mutants fail to develop flowers (Schultz and Haughn, 1991, Huala and Sussex, 1992, Weigel *et al.*, 1992).

LFY mutations have limited effects on bracts (lemmas in grasses) or on the outermost floral whorls, including sepals in Arabidopsis and paleas in grasses (Fig. 2F). In Arabidopsis, weak *lfy* mutant, petals are transformed into small sepals or mosaic organs including sepal and petal tissue (Huala and Sussex, 1992, Weigel *et al.*, 1992). Lodicules in grasses are homologous to eudicot petals (Yoshida, 2012), and *lfy* mutants show reduced number and altered morphology of lodicules, which include transformation into bracts and fusions with stamens both in wheat (Fig. 2F) and rice (Ikeda-Kawakatsu *et al.*, 2012). In addition, *LFY* mutants show reduced number of stamens and increased number of carpels in wheat (Fig. 2F), rice (Ikeda-Kawakatsu *et al.*, 2012), and Arabidopsis (Huala and Sussex, 1992). One stamen and three carpels were observed frequently in the wheat *lfy* mutant (Fig. 2F), suggesting homeotic conversions from stamens to carpels.

In spite of the similar roles of *LFY* in floral organ development, there are also important differences in other *LFY* functions between Arabidopsis and grasses. First, strong *lfy* mutations in Arabidopsis result in the replacement of most flowers by shoots subtended by cauline leaves and the few observed late flowers have intermediate inflorescence characteristics (Schultz and Haughn, 1991, Weigel *et al.*, 1992). By contrast, flowers initiate normally in the *lfy* mutants in wheat (Fig. 2F) and other grasses (Bomblies *et al.*, 2003, Ikeda-Kawakatsu *et al.*, 2012), and defects appear only later at the inner floral whorls. These results indicate that *LFY* is required to confer the initial floral meristem identity in Arabidopsis but not in the grasses.

The previous difference, likely affects the opposite functions of *LFY* in inflorescence development in these species. In Arabidopsis, constitutive expression of *LFY* (*35S:LFY*) results in conversion of both apical and axillary meristems into terminal flowers, demonstrating that *LFY* is a limiting factor defining when and where flowers are produced (Weigel and Nilsson, 1995). By contrast, constitutive expression of *LFY* in wheat increases the number of lateral spikelets, likely by delaying the IM>TS transition (Fig. 3). Mutations in *LFY* also result in opposite effects in eudicots and grasses. Weak *lfy* mutants delay the formation of flowers and increase the number of secondary branches in Arabidopsis and other eudicot species (Coen *et al.*, 1990, Schultz and Haughn, 1991, Weigel *et al.*, 1992, Souer *et al.*, 1998, Molinero-Rosales *et al.*, 1999). In contrast, *LFY* loss-of-function mutations result in significant reductions in SNS in wheat (Fig. 2), and in the number of branches in rice panicles (Ikeda-Kawakatsu *et al.*, 2012) and maize male inflorescences (Bomblies *et al.*, 2003). These results indicate that in grasses, *LFY*

promotes indeterminate growth and prevents the precocious formation of terminal spikelets, whereas in Arabidopsis it promotes the formation of flowers.

In summary, *LFY* has a similar role on floral organ development in Arabidopsis and grasses, but different roles in floral meristem identity and inflorescence meristem determinacy.

Interactions between LFY and WAPO1 are critical for their functions

LFY and WAPO1 proteins physically interact with each other in wheat (Fig. 4), barley (Selva *et al.*, 2021), rice (Ikeda-Kawakatsu *et al.*, 2012) and Arabidopsis (Chae *et al.*, 2008). In Arabidopsis, UFO interaction with LFY modifies its DNA binding specificity and alters the set of genes directly regulated by LFY (Rieu *et al.*, 2023). For example, the LFY-UFO interaction is required for the correct activation of *AP3* during Arabidopsis flower formation (Levin and Meyerowitz, 1995, Wilkinson and Haughn, 1995, Lee *et al.*, 1997).

The simultaneous presence of *WAPO1* and *LFY* is also required for the correct regulation of floral organ identity genes and normal flower development in the grasses. Loss-of-function mutations in *LFY* in barley (Selva *et al.*, 2021) and *WAPO1* in wheat (Kuzay *et al.*, 2022) result in the downregulation of common class-B (*AP3* and *PI-1*), class-C (*AG1*) and class-E (*SEP3.2*) floral organ identity genes, which likely explains the similar floral defects observed in the *lfy* (Fig. 2) and *wapo1* mutants (Kuzay *et al.*, 2022) in these species.

In Arabidopsis, *ufo* mutants show only small (but still significant) increases in the number of secondary branches (Levin and Meyerowitz, 1995). By contrast, the *wapo1* mutant in wheat shows similar reductions in SNS as the *lfy* and *lfy wapo1* combined mutants (Fig. 7A). Similar reductions in the number of panicle branches are also observed in the *apo1*, *apo2* and combined *apo1 apo2* mutants in rice (Ikeda-Kawakatsu *et al.*, 2012). These results suggest that the physical interaction between LFY and WAPO1 likely plays a more prominent role in the regulation of IM determinacy in grasses than in the regulation of flower initiation in Arabidopsis.

Interactions between *LFY* and *SQUAMOSA* genes modulate their opposite effects on IM determinacy

MADS-box transcription factors act as master regulators of developmental switches and organ specification, with meristem identity genes from the *SQUAMOSA* clade playing essential roles in the initiation of flower development. In the wheat *vrn1 ful2 ful3* combined mutant, lateral

spikelets are completely transformed into vegetative tillers subtended by leaves (Li *et al.*, 2019), whereas in the Arabidopsis *ap1 cal ful* triple mutant flowers are transformed into leafy shoots (Ferrándiz *et al.*, 2000). In Arabidopsis, *AP1* orchestrates floral initiation by directly regulating hundreds of genes (Kaufmann *et al.*, 2010), which is favored by AP1 ability to modulate chromatin accessibility of its target genes (Pajoro *et al.*, 2014). *LFY* is also a pioneer transcription factor that can regulate hundreds of genes by contacting its cognate binding motifs even in closed chromatin (Jin *et al.*, 2021).

In Arabidopsis, *LFY* positively regulates the expression of *AP1* and *CAL* (Wagner *et al.*, 1999, William *et al.*, 2004) and, therefore, indirectly regulates their direct targets. *LFY* also directly regulates hundreds of genes independently of *AP1* and *CAL* (Goslin *et al.*, 2017). However, induction of *LFY* in *ap1 cal* mutants is insufficient to rescue the very limited and late formation of flowers observed in this double mutant. In addition, induction of *LFY* results in a lower proportion of plants with flowers than in the control without *LFY* induction (Goslin *et al.*, 2017). These results indicate that, in the absence of *AP1* and *CAL, LFY* can inhibit flower formation in Arabidopsis, similar to the normal function of *LFY* in the grass species. These results also suggest that the different roles of *LFY* in the direct regulation of the *SQUAMOSA* genes between Arabidopsis and grasses likely contribute to the opposite functions of *LFY* in the regulation of the IM determinacy between these species.

Approximately 200 genes have been identified in Arabidopsis as high-confidence direct targets of both LFY and AP1 (Winter *et al.*, 2015). Although many of the shared genes directly regulated by the induction of *AP1* or *LFY* show changes in expression with identical directionality, some of them are regulated in opposite directions, including several key regulators of floral initiation (Goslin *et al.*, 2017). These common gene targets can contribute to the epistatic interactions between LFY and AP1 and to their ability to coordinate the transcriptional programs required for flower initiation and early flower development in Arabidopsis.

Genes directly regulated by *LFY* and *SQUAMOSA* genes are likely to exist also in wheat and may contribute to the significant genetic interaction for SNS observed between *LFY* and *VRN1* in this study (Fig. 8A). However, our Y1H assays suggest that direct interactions between LFY and a *VRN1* promoter region including a predicted LFY binding site can also contribute to the observed genetic interaction for SNS. This hypothesis is also supported by the significant effect

on *VRN-A1* transcript levels and SNS of one EMS induced mutation within this predicted LFY binding site in the *VRN1* promoter (Zhang *et al.*, 2023b). Regardless of the relative contributions of direct and indirect interactions to the significant genetic interaction for SNS between *LFY* and *VRN1*, it is important to point out that this interaction explains only a small proportion of the variation in SNS in this experiment (Table S19). Whereas the maximum effects of *VRN1* and *LFY* were 9.2 and 10.4 spikelets per spike, respectively, the net effect of the interaction was limited to 5.2 spikelets per spike (Table S19).

Spatio-temporal expression patterns "illuminate" *LFY* and *WAPO1* function

LFY expression. Since the beginning of spike development *LFY* expression was not uniform, with high expression levels at the leaf ridge and low levels or no expression at the spikelet ridge (Fig. 5B-C), a pattern observed previously by *in situ* hybridization (Shitsukawa *et al.*, 2006). *LFY* expression in the young SMs also delimited a proximal region with high levels of expression from a distal region with low or no *LFY* expression (Fig. 5B-C). A similar pattern was also observed in the SMs in young barley spikes (Zhong *et al.*, 2021) and in the primary and secondary branch meristems in the developing panicles in rice (Kyozuka *et al.*, 1998, Miao *et al.*, 2022), suggesting a conserved function in grasses. We hypothesize that the regions of low *LFY* expression contribute to the delimitation of the areas where the new wheat spikelets or panicle branches will be formed.

As the spikes approached the IM>TS transition (W3.25), a significant reduction of *LFY* transcript levels relative to previous stages was observed in the distal part of the spike, including the IM and adjacent young SMs (Fig. 5, Table S14). Based on *LFY*'s role in maintaining IM indeterminacy in wheat and other grasses, we hypothesize that that the reduced expression of *LFY* in the distal part of the spike may be an early indication of the IM>TS transition.

The expression profiles of *LFY* during spikelet development also provided insights on its role in the regulation of the inner floral organs. At W3.25, the region of the developing spikelets distal to the lemma primordia, become divided in a narrow nest-shaped proximal region with very high *LFY* expression and a distal region with low or no *LFY* expression (Fig. 5D). This spatial differentiation seems to be biologically relevant since *WAPO1* and several floral organ identity genes were preferentially expressed in the distal region with limited *LFY* expression (Fig. 6).

In summary, the dynamic *LFY* spatio-temporal expression patterns during wheat spike and floral development reflect different *LFY*'s functions and are likely to carry useful spatial information for the regulation of downstream genes.

WAPO1 expression. The spikelet maturation gradient from the distal to the central part of the wheat spike, provides a useful developmental time series. *WAPO1* expression (Fig. 5 and S5) was detected in younger spikelets than class-B (*AP3* and *PI-1*), class-C (*AG1* and *AG2*) (Fig. 6) and class-E (*SEP3.1* and *SEP3.2*, Fig. S8) floral organ identity genes, suggesting that *WAPO1* is expressed earlier. Many of the floral organ identity genes are significantly downregulated in the *wapo1* mutant in wheat (Kuzay *et al.*, 2022) and the *lfy* mutant in barley (Selva *et al.*, 2021), suggesting that *LFY* and *WAPO1* are both important for their correct regulation.

The adjacent expression domains of *LFY* and *WAPO1* in the developing spikelet generate a curved region of contact (Fig. 5D), where proteins encoded by these two genes have a higher opportunity to interact with each other. Based on the Arabidopsis results from Rieu *et al.* (2023), we hypothesize that within this dynamic overlap region WAPO1 redirects LFY to a different set of gene targets than the ones regulated by LFY alone, providing important spatial information for the correct regulation of the floral organ identity genes. In addition, the common floral defects observed in the *lfy* and *wapo1* mutants, indicate that this spatial information is critical for the normal development of the floral organs in the multiple florets formed within each of the wheat spikelets.

Given the strong genetic interactions for SNS between *WAPO1* and *LFY* (Fig. 7A), we initially thought that *WAPO1* would be expressed in the IM close to the time of the IM>TS transition, similarly to what we observed for *LFY*. Although the expression of both genes overlapped in the IM at the initial stages of spike development (W1.5), *WAPO1* transcripts were restricted to the basal - central region of the developing spike at later stages (Fig. 5 and S5). Two non-mutually exclusive hypothesis may explain this discrepancy with our original hypothesis. First, *WAPO1* is expressed at much lower levels than *LFY* (Fig. S5), so it is still possible that *WAPO1* is expressed in the IM but below our current detection threshold. Alternatively, the expression of *WAPO1* at the base of the developing spike at the differentiating vascular tissue may suggest transport of the WAPO1 protein to the IM, a hypothesis that needs to be tested experimentally.

VRN1 and FUL2 expression. Since *LFY* and *WAPO1* function as repressors of the IM>TS transition, we initially hypothesized that they could work as repressors of *VRN1/FUL2* in the IM, releasing them at the time of the IM>TS transition. However, we did not observe any changes in the expression of *VRN1*, *FUL2* (Fig. 6D) or *FUL3* (Fig. S7) in the IM during spike development, suggesting that our initial hypothesis is likely incorrect.

The uniform distribution of *VRN1* and *FUL2* expression through the developing spike suggest that other genes are required to provide the spatial information required for VRN1 and FUL2 functions on SNS and spikelet development. In addition, the high levels of expression of *VRN1* and *FUL2* in the IM at all stages of spike development suggest that, additional genes may be required to prevent a premature formation of the terminal spikelet. Interestingly, several of the recently cloned genes affecting SNS in wheat operate as repressors of the IM>TS transition including *LFY* (this study), *WAPO1* (Kuzay *et al.*, 2022), *bZIPC1* (Glenn *et al.*, 2023) and *SPL17* (Liu *et al.*, 2023) (Fig. S10), with mutants for all these genes resulting in reduced SNS. In summary, these results suggest that multiple regulatory mechanisms may exist in wheat to balance the high expression levels of *VRN1* and *FUL2* in the IM and to adjust the timing of the IM>TS transition to optimize the SNS to the available resources.

Developmental studies of the wheat spike have valuable practical implications

Selection for variation in *VRN1* is a possible target for SNS improvement, but the strong pleiotropic effects of mutations in this gene on heading time (Yan *et al.*, 2003) complicate the utilization of natural or induced *VRN1* variants for SNS improvement. To avoid these pleiotropic effects recent efforts have been concentrated in the identification of genes with natural variants affecting SNS but with limited effects on heading time.

A recent example is the natural D10A polymorphism identified in the FT-A2 protein in wheat, which showed positive effects on SNS, grain number per spikes, and grain weight per spike, with limited effects on heading time. The derived *FT-A2* allele associated with increased SNS (A10) showed evidence of positive selection in modern hexaploid wheat (Glenn *et al.*, 2022). FT2 physically interacts with bZIPC1, which also showed natural variation in wheat associated with differences in SNS, and evidence of positive selection in modern wheat varieties (Glenn *et al.*, 2023). Genetic interactions for SNS were detected between natural variants of *FT-A2* and

bZIPC-B1, with alleles resulting in the optimum combinations for SNS showing simultaneous frequency increases in modern wheat varieties (Glenn *et al.*, 2023).

In this study, we observed frequency increases in hexaploid wheat of the *LFY-B* allele P+,34L,80S (Fig. 1D), which parallel those described previously for the *WAPO-A1* allele 47F (Kuzay *et al.*, 2019, Kuzay *et al.*, 2022). We also showed that, when combined, these two alleles showed favorable effect on SNS (Fig. 7B). Taken together the *FT-A2*/*bZIPC-B1* and *LFY-B/WAPO-A1* interaction results, suggest that alleles showing significant genetic and physical interactions are likely to be simultaneously affected by natural and/or human selection.

Wheat breeders usually select lines for higher grain yield, large spikes, and/or spikes with more grains, exerting a strong selection pressure on genes controlling the IM>TS transition. This pressure has resulted in gradual increases in the frequencies of alleles or allele combinations that favor SNS increases. However, the acceleration of current rates of yield improvement will require a better understanding of the gene networks that regulate SNS to engineer optimal allele combinations across multiple genes. This study highlights the value of combining developmental and genetic studies to identify optimal allele combinations for grain yield components in a crop species that is critical for our global food security.

Acknowledgements

We would like to thank Stephen Pearce (Rothamsted Research) and Youngjun Mo (JeonBuk National University) for identifying the *LFY-B* mutant, developing markers and the initial backcrossing to Kronos. We thank Maria von Korff (Heinrich Heine University Düsseldorf) for a valuable revision of the manuscript and for her supervision of Tianyu Lan. We also thank Dr. Kun Li (UC Davis) for her help with multiple experiments.

Competing Interests

No competing interests declared

Funding

This project was supported by the Agriculture and Food Research Initiative Competitive Grants 2022-67013-36209 and 2022-68013-36439 (WheatCAP) from the United States Department of Agriculture National Institute of Food and Agriculture and by the Howard Hughes Medical

Institute. D.P.W. was a Howard Hughes Medical Institute Fellow of the Life Sciences Research Foundation (http:// www.lsrf.org/). The funders played no role in this research beyond providing the funding.

Author contributions

FP, JZ and HL performed most of the experimental work and contributed to data analysis. FP provided the first version of the paper except for the natural variation section that was provided by JZ. HL led the smFISH experiment. CL contributed the transgenic plants, performed the Y1H, and supervised HL. TL and AJ contributed to several experiments. DW and JMD supervised FP, helped to characterize the mutants and transgenic lines, and contributed to the design of several experiments. JD designed and coordinated the project, obtained funding, supervised the research team, performed statistical analyses, and wrote the final version of the manuscript. All authors contributed to the writing and revision of the manuscript.

Data Availability

All data generated during this study and the corresponding statistical analyses are included the supporting Excel file. Kronos mutants are available from the authors upon request without any restrictions for use and from the Germplasm Resources Unit (GRU) at the John Innes Centre. Images for the spike sections used in the smFISH and hybridization coordinates for the genes presented in this study are available at https://dubcovskylab.ucdavis.edu/content/spatial-transcriptomic.

Materials and Methods

Plant Materials

We first tested if natural variation in the chromosome regions including *LFY-A* and *LFY-B* were associated with differences in spikelet number per spike (SNS), to determine the agronomic potential of a study including these genes. We reanalyzed a set of nested association mapping populations that were previously characterized for this trait in three field experiments under full and limited irrigation at the University of California, Davis between 2014 and 2016 (Zhang *et al.*, 2018). We only detected significant differences in SNS associated with the *LFY-B* region in one of the populations (Berkut x PBW343). To validate this association, we developed

heterogeneous inbred families (HIFs) from two F_5 lines (SSD40 and SSD63) from this population that were still heterozygous for the *LFY-B* region, and evaluated them for SNS.

To confirm the linkage between *LFY-B* and the QTL for SNS, we screened 385 $F_{5:3}$ lines (770 chromosomes) segregating for the *LFY-B* region for recombination events between flanking markers 2B-657.1 (2B: 657,072,439) and 2B-660.1 (660,114,463, Table S5). We genotyped the recombinant lines with six additional markers developed within this region (Table S5) and identified three $F_{5:2}$ lines heterozygous for *LFY-B* with close recombination events at both sides of *LFY-B* (Table S7). From the progeny of these lines, we selected 10 $F_{7:2}$ plants homozygous for the recombinant chromosome and 10 sister plants homozygous for the non-recombinant chromosome, carrying the alternative *LFY-B* alleles. We evaluated the $F_{7:3}$ progeny of these 20 lines as single 1m rows in the field in 2021, at the UC Davis Experimental Station.

Natural variation and haplotype analysis

We performed a haplotype analysis for an 813.4 kb region of chromosome 2B including *LFY-B* (657,790,878 to 658,604,020 in CS RefSeq v1.1) using exome capture data from 56 common and pasta wheat accessions (https://wheat.triticeaetoolbox.org/downloads/download-vcf.pl) generated by the WheatCAP project (Exome_Capture_2017_WheatCAP_UCD). To obtain the complete *LFY* sequences associated to the different haplotypes, we assigned the different wheat sequenced genomes (Avni *et al.*, 2017, Maccaferri *et al.*, 2019, Walkowiak *et al.*, 2020, Sato *et al.*, 2021) to the haplotypes identified in the previous analysis.
The previous analysis revealed four polymorphisms among the different *LFY* alleles, for which we developed molecular markers. We used these markers to screen a wheat germplasm collection including 85 *T. turgidum* ssp. *dicoccoides*, 86 *T. turgidum* ssp. *dicoccon*, 384 *T. turgidum* ssp. *durum*, and 234 *T. aestivum* accessions, which are part of a photoperiod insensitive spring wheat panel from North America previously evaluated for multiple agronomic traits (Zhang *et al.*, 2018).

Epistatic interactions between natural variants of *LFY-B* and *WAPO-A1*

To evaluate the combined effect of the natural variants in *LFY-B* and *WAPO-A1*, we characterized two hexaploid and two tetraploid populations segregating for both genes. For *WAPO-A1*, we focused on the C47F amino acid change which was previously shown to be

associated with significant differences in SNS (Kuzay *et al.*, 2022). The first hexaploid population, Berkut x RAC875, included 75 RILs that were previously evaluated for SNS in six different environments (Zhang *et al.*, 2018). The second hexaploid population, RSI5 x RAC875, was evaluated in three separate experiments, first as F_2, then as $F_{2:2}$ plants derived from F_2 plants heterozygous for *LFY-B* and *WAPO-A1*, and finally as $F_{3:2}$ plants derived from F_3 plants heterozygous for both genes. Plants homozygous for the four possible *LFY-B/WAPO-A1* allele combinations were selected with molecular markers and evaluated for SNS. Average SNS was calculated from two spikes per plant from the two taller tillers.

For the first tetraploid population, we crossed Kronos x Gredho (which carried the desired *LFY-B* allele) and then backcrossed it to a Kronos line in which we have previously introgressed the *WAPO-A1* 47F allele from hexaploid wheat (Kuzay *et al.*, 2022). We backcrossed this plant four times to the Kronos-47F line, selecting in each generation plants heterozygous for both genes using molecular markers. Finally, we generated BC_4F_2 seeds from a single BC_4F_1 plant heterozygous for both genes and planted it in the field at UC Davis in November 2022 as single plants. The second population was generated from the cross between Kronos and an unusual durum line from Syria (PI 519639) which carried the desired *LFY-B / WAPO-A1* allele combination. The F_1 was backcrossed once to Kronos, and one BC_1F_3 plant heterozygous for both alleles was used to generate $BC_1F_{3:2}$ plants that were grown in the UC Davis field for SNS evaluation. We genotyped both populations using molecular markers, and evaluated the mature plants homozygous for the four different *LFY-B/ WAPO-A1* combinations in 2023 for SNS using three spikes per plant.

Ethyl methanesulfonate (EMS) induced mutants

We screened the sequenced tetraploid wheat variety Kronos population (Krasileva *et al.*, 2017) by BLASTN to identify loss-of-function mutations in the *LFY-A1* and *LFY-B1* homeologs. To reduce background mutations, the *lfy-B* mutant was backcrossed twice to Kronos and then to the *lfy-A* mutant. The double mutant was backcrossed once to Kronos and in the progeny homozygous sister lines were selected for the four possible homozygous combinations, including the *lfy-A lfy-B* combined mutant (henceforth, *lfy*). This line is BC_1 for *lfy-A* and BC_2 for *lfy-B* so it is referred to as $BC_{1\text{-}2}$. Genome specific markers for the *lfy-A* and *lfy-B* mutations were

designed and used to genotype plants during backcrossing and combination with other mutations described below. Primers are listed in Table S5.

The *lfy* mutant was intercrossed with Kronos lines developed in previous studies homozygous for loss-of-function EMS mutations in the A and B genomes of *VRN1* (Chen and Dubcovsky, 2012) and *FUL2* (Li *et al.*, 2019), and for CRISPR generated loss-of-function mutations in *WAPO1* (Kuzay *et al.*, 2022), to generate higher order mutant combinations. These lines had at least two backcrosses to the parental line Kronos to reduce the number of background mutations. For these crosses we used a line heterozygous for one of *LFY* mutation to restore fertility.

Plant growth and phenotypic characterization

Plants were stratified for 2-days at 4 °C in the dark and then planted in growth chambers (PGR15, Conviron, Manitoba, Canada). Lights were set to 350 µmol m^{-2} s^{-1} at plant level. Plants were grown under inductive 16-hour long days with temperatures set during the day to 22°C and during the night to 17°C. Relative humidity in growth chambers was maintained at 60-70% throughout the duration of the experiments. Heading time was recorded as the number of days from germination to full emergence of the spike from the leaf sheath, and that time the spikelet number per spike (SNS) was measured from the main tiller.

Generation of the wheat transgenic lines overexpressing *LFY*

We cloned the *LFY-A* coding regions by PCR from cDNA derived from Kronos developing spikes using primer LFY-A-GW-F combined with either LFY-A-GW-R1 (with no tag) or LFY-A-GW-R2 (with an HA tag) listed in Table S5. We then recombined it into pDONR/zeo entry vector using Life Technologies BP Clonase II following the manufacturer's protocol. The pDONR/zeo vector containing the *LFY-A* coding region was next recombined into the Japan Tobacco pLC41 vector downstream of the maize *UBIQUITIN* promoter using Life Technologies LR Clonase II to generate two constructs: one expressing *LFY* with a C-terminal 3xHA tag, and the other without a tag. Clones were verified by Sanger sequencing at each cloning step. The two T-DNA binary constructs were transformed into wheat variety Kronos using *Agrobacterium*-mediated transformation (EHA105) at the UC Davis Plant Transformation Facility as described before (Debernardi *et al.*, 2020b). The presence of the *LFY* transgene was determined with primers LFY-Genotyping-R5 and UBI-F2 listed in Table S5.

LFY transcript levels were determined by qRT-PCR using primers LFY_qPCR_F and LFY_qPCR_R and *ACTIN* as endogenous control (Table S5). For qRT-PCR experiments, RNA was extracted using the Spectrum Plant Total RNA Kit (Sigma-Aldrich, St. Louis, MO, USA) or as previously described by (Ream *et al.*, 2014). One µg of RNA was treated with RQ1 RNase-Free DNase (Promega, M6101) first and then used for cDNA synthesis with the High-Capacity cDNA Reverse Transcription Kit (Applied Biosystems, Foster City, CA, USA). The qRT-PCR experiments were performed using Quantinova SYBR Green PCR kit (Qiagen, 208052) in a 7500 Fast Real-Time PCR system (Applied Biosystems). Transcript levels for all genes are expressed as linearized fold-*ACTIN* levels calculated by the formula $2^{(ACTIN\ C_T - TARGET\ C_T)} \pm$ standard error (SE) of the mean.

Single-molecule fluorescence *in-situ* hybridization (smFISH)

We used the Molecular Cartography™ technology from Resolve BioSciences combinatorial smFISH. Wheat shoot apical meristems were collected from the vegetative to the spike lemma primordia stage. The samples were immediately fixed in 4% PFA after harvest, dehydrated, and embedded in paraffin. Sections from the central plane of the developing spikes (10µm-thick) were placed on the slides and dried overnight at 37°C, followed by a 10-minute bake at 50°C. The sections were then deparaffinized, permeabilized, and refixed according to the user guide. After complete dehydration, the sections were mounted using SlowFade-Gold Antifade reagent, covered with a thin glass coverslip, and sent to Resolve BioSciences on dry ice for analysis as described in our previous study (Glenn *et al.*, 2023).

Probes were designed using Resolve BioSciences' proprietary design algorithm and gene annotations from Chinese Spring RefSeqv1.1. To identify potential off-target sites, searches were confined to the coding regions. Each target sequence underwent a single scan for all k-mers, favoring regions with rare k-mers as seeds for full probe design. For each of the wheat genes selected for smFISH probe design (Table S15), we targeted the homoeolog expressed at higher levels in a Kronos transcriptome including different stages of spike development (VanGessel *et al.*, 2022), and provided Resolve BioSciences their respective homeologs to be excluded in their quality control for specificity performed against all the coding sequences of the wheat genome (Ref Seq v1.1). Therefore, probes are not genome-specific and may detect both homoeologs for each gene (Catalogue No. PGGS, all these probes are part of kit number K7128).

Imaging and image processing was performed as described before (Glenn *et al.*, 2023). Final image analysis was performed in ImageJ using the Polylux tool plugin from Resolve BioSciences to examine specific Molecular Cartography™ signals.

Co-immunoprecipitation (Co-IP) assay and western blotting

To test the physical interaction between WAPO and LFY, we performed a co-IP experiment in wheat leaf protoplasts using a method described previously (Zhang *et al.*, 2023a), with minor modifications. The *WAPO1* coding region was initially synthesized by Genewiz into the pUC57 vector, amplified with primers WAPO1_BP_F and WAPO1_BP_R (Table S5), cloned into pDONR/zeo vector using Life Technologies BP Clonase II, and recombined into the Japan Tobacco pLC41 vector downstream of the maize *UBIQUITIN* promoter with a C-terminal 4xMYC tag (for transgenic experiments). Next, we switched both *UBI:WAPO1-MYC* and *UBI:LFY-HA* from the pLC41 binary vector to the smaller pUC19 vector to enhance the transfection efficiency of the protoplasts. The *UBI:WAPO-MYC* and *UBI-LFY-HA* DNA fragments were cleaved using restriction enzymes *Hind*III and *Spe*I, gel purified, and then ligated with the *Hind*III-*Xba*I linearized pUC19 vector (*Spe*I and *Xba*I create compatible ends). Both constructs were verified by restrictions and Sanger sequencing.

We transformed Kronos leaf protoplasts with and 50 µg of each *UBI:LFY-HA* and *UBI: WAPO1-MYC* in 50 ml tubes containing 2 ml of protoplast (roughly 0.5 x 10^6 cell per mL). As negative controls, we performed separate transformations including only one of the two plasmids. After transformation, protoplasts were resuspended in 5 ml W5 buffer and incubated in a 6-well plate at room temperature overnight. Total protein was extracted with 1 ml of IP lysis buffer (25 mM Tris-HCl pH7.5, 150 mM NaCl, 1 mM EDTA, 1% NP-40 substitute, 5% glycerol and 1 x Protease Inhibitors). Part of the protein extract were set aside as input control (50 µl), and the rest was used for co-immunoprecipitation using Pierce Anti-HA Magnetic Beads (ThermoFisher Cat. 88836) by gentle agitation on a tube rotator for 30 min at room temperature with additional 1x proteinase inhibitors. Proteins were eluted by boiling the beads in 50 µl 1x Laemmli sample buffer for 10 min.

For Western Blot, half of the Co-IP elution and 50 µg of input for each sample were loaded onto a 12% SDS-PAGE gel. After protein was transferred to a PVDF membrane using the Bio-Rad Trans-Blot Turbo Transfer System (Cat. 1704150), the membrane was blocked with 1x TBST

buffer containing 5% non-fat milk for 1 h at room temperature. Anti-cMyc-peroxidase monoclonal antibody (Roche 11814150001) was added at a dilution of 1:10,000 and was incubated at room temperature for 1h. After four 10 min washes using 1x TBST buffer, the signals were developed using SuperSignal West Femto Maximum Sensitivity Substrate (ThermoFisher, Cat. 34096). After imaging, the membrane was stripped with mild stripping buffer (1.5% glycine, 0.1% SDS, 1% Tween 20, pH 2.2), re-blocked for 1 h at RT, and then probed with anti-HA-peroxidase at a dilution of 1:2500 (Roche 12013819001) for 1 h at room temperature.

Yeast-one-hybrid (Y1H)

We previously identified a mutation in a conserved nucleotide of a predicted *LFY* binding site in the *VRN-A1* promoter in chromosome 5A: 587,423,515 (CS RefSeq v1.0) in Kronos mutant K2944. This mutation was associated with differences in *VRN1* expression and SNS (Zhang *et al.*, 2023b), so we performed a Y1H experiment using the Matchmaker® Gold One-Hybrid System (Takara) to test the ability of LFY to bind to this predicted site. A DNA segment from the *VRN-A1* promoter (-328 to -221 bp upstream of the start codon) including a putative LFY binding site (CCAATGG) was amplified by PCR using primers VRN1-SacI-F and VRN1-XhoI-R (Table S5). The fragment was cloned using IN-Fusion HD cloning kit (Takara) into a *Sac*I-*Xho*I linearized pAbAi vector upstream of the *AUR1-C* reporter gene (Aureobasidin A resistance) to generate the bait vector. After quality control by Sanger sequencing, the bait vector containing the *VRN1* promoter was linearized with *BstB*I restriction enzyme and integrated into the genome of Y1H gold yeast to generate the *VRN1*-bait strain. We next determined that 750 ng/ml of AbA was sufficient to significantly suppress the basal *AUR1-C* expression of the *VRN1*-bait, and used 750, 1000 and 1250 ng/ml of AbA for subsequent bait-prey interaction tests. The coding region of LFY was PCR amplified using primers LFY-NdeI-F and LFY-EcoRI-R (Table S5) and inserted into the pGADT7 prey vector between *Nde*I and *EcoR*I restriction sites to generate the prey construct. The LFY-pGADT7 prey was transformed into *VRN1*-bait yeast cells following the manufacturer's protocol (Matchmaker® Gold One-Hybrid System, Takara), and the empty vector pGADT7 was also transformed into *VRN1*-bait cells and used as negative control. Dilution series (1:10 and 1:100) of yeast cells transformed with LFY-pGADT7 or pGADT7 were plated on minimal synthetic defined (SD) medium lacking Leucine (SD-Leu),

and SD medium lacking Leu supplemented with 750 ng/ml, 1000 ng/ml, or 1250 ng/ml AbA antibiotics, and grown at 30°C for four days.

Supplementary figures

Fig. S1. Alignment of LFY proteins from multiple grass species.

Fig. S2. Effect of individual and combined *LFY* mutants on spikelet number per spike (SNS).

Fig. S3. *LFY* transcript levels in transgenic plants overexpressing *LFY*.

Fig. S4. Expression analysis of *LFY* and *WAPO1.*

Fig. S5. Single-molecule fluorescence *in situ* hybridization (smFISH) for *WAPO1.*

Fig. S6. Effect of *lfy* mutants on *VRN1* and *FUL2* expression.

Fig. S7. Single-molecule fluorescence *in situ* hybridization (smFISH) for *FUL3.*

Fig. S8. Single-molecule fluorescence in situ hybridization (smFISH) for *SEPALLATA* genes.

Fig. S9. Yeast-one-hybrid (Y1H) assay between LFY and the *VRN-A1* promoter.

Fig. S10. Simplified working model of the regulation of SNS in wheat.

Supplementary Tables

Table S1. SNS QTL linked to *LFY-B* in the Berkut x PBW343 segregating RIL population.

Table S2. Supporting data for Fig. 1A and C.

Table S3. Haplotype analysis of the *LFY-B* region.

Table S4. *LFY-B* haplotypes in wheat varieties sequenced in the pangenome project.

Table S5. Primers used in this study.

Table S6. Frequency of the different *LFY-B* alleles in tetraploid and hexaploid wheat.

Table S7. Supporting data Fig. 1E.

Table S8. Genes annotated in the candidate gene region for the SNS QTL.

Table S9. Supporting data for Fig. 2C-E.

Table S10. Supporting data for Fig. S2.

Table S11. Supporting Data for Fig. S3.

Table S12. Supporting data for Fig. 3.

Table S13. Supporting data for Fig. S4.

Table S14. *LFY* transcripts density at the distal region of the developing spike.

Table S15. Genes used in the sm-FISH experiments.

Table S16. Supporting data for Fig. S6.

Table S17. Supporting data for Fig. 7A.

Table S18. Supporting data for Fig. 7B-D.

Table S19. Supporting data for Fig. 8.

References

Alvarez, M.A., Tranquilli, G., Lewis, S., Kippes, N. and Dubcovsky, J. (2016) Genetic and physical mapping of the earliness *per se* locus *Eps-A*^{m}*1* in *Triticum monococcum* identifies *EARLY FLOWERING 3* (*ELF3*) as a candidate gene. *Funct Integr Genomic*, **16**, 365-382.

Avni, R., Nave, M., Barad, O., Baruch, K., Twardziok, S.O., Gundlach, H., Hale, I., Mascher, M., Spannagl, M., Wiebe, K., Jordan, K.W., Golan, G., Deek, J., Ben-Zvi, B., Ben-Zvi, G., Himmelbach, A., MacLachlan, R.P., Sharpe, A.G., Fritz, A., Ben-David, R., Budak, H., Fahima, T., Korol, A., Faris, J.D., Hernandez, A., Mikel, M.A., Levy, A.A., Steffenson, B., Maccaferri, M., Tuberosa, R., Cattivelli, L., Faccioli, P., Ceriotti, A., Kashkush, K., Pourkheirandish, M., Komatsuda, T., Eilam, T., Sela, H., Sharon, A., Ohad, N., Chamovitz, D.A., Mayer, K.F.X., Stein, N., Ronen, G., Peleg, Z., Pozniak, C.J., Akhunov, E.D. and Distelfeld, A. (2017) Wild emmer genome architecture and diversity elucidate wheat evolution and domestication. *Science*, **357**, 93-97.

Bomblies, K., Wang, R.L., Ambrose, B.A., Schmidt, R.J., Meeley, R.B. and Doebley, J. (2003) Duplicate *FLORICAULA/LEAFY* homologs *zfl1* and *zfl2* control inflorescence architecture and flower patterning in maize. *Development*, **130**, 2385-2395.

Chae, E., Tan, Q.K.G., Hill, T.A. and Irish, V.F. (2008) An Arabidopsis F-box protein acts as a transcriptional co-factor to regulate floral development. *Development*, **135**, 1235-1245.

Chen, A. and Dubcovsky, J. (2012) Wheat TILLING mutants show that the vernalization gene *VRN1* down-regulates the flowering repressor *VRN2* in leaves but is not essential for flowering. *PLoS Genet*, **8**, e1003134.

Choulet, F., Alberti, A., Theil, S., Glover, N., Barbe, V., Daron, J., Pingault, L., Sourdille, P., Couloux, A., Paux, E., Leroy, P., Mangenot, S., Guilhot, N., Le Gouis, J., Balfourier, F., Alaux, M., Jamilloux, V., Poulain, J., Durand, C., Bellec, A., Gaspin, C., Safar, J., Dolezel, J., Rogers, J., Vandepoele, K., Aury, J.M., Mayer, K., Berges, H., Quesneville, H., Wincker, P. and Feuillet, C. (2014) Structural and functional partitioning of bread wheat chromosome 3B. *Science*, **345**, 1249721.

Coen, E.S., Romero, J.M., Doyle, S., Elliott, R., Murphy, G. and Carpenter, R. (1990) *Floricaula* - a homeotic gene required for flower development in *Antirrhinum majus*. *Cell*, **63**, 1311-1322.

Debernardi, J.M., Greenwood, J.R., Jean Finnegan, E., Jernstedt, J. and Dubcovsky, J. (2020a) *APETALA 2*-like genes *AP2L2* and *Q* specify lemma identity and axillary floral meristem development in wheat. *Plant J.*, **101**, 171-187.

Debernardi, J.M., Tricoli, D.M., Ercoli, M.F., Hayta, S., Ronald, P., Palatnik, J.F. and Dubcovsky, J. (2020b) A GRF-GIF chimeric protein improves the regeneration efficiency of transgenic plants. *Nat. Biotechnol.*, **38**, 1274-1279.

FAOSTAT (2017) http://www.fao.org/faostat/en/#data: Food and Agriculture Organization (FAO) of the United Nations.

Ferrándiz, C., Gu, Q., Martienssen, R. and Yanofsky, M.F. (2000) Redundant regulation of meristem identity and plant architecture by *FRUITFULL*, *APETALA1* and *CAULIFLOWER*. *Development*, **127**, 725-734.

Frank, A.B. and Bauer, A. (1982) Effect of temperature and fertilizer-N on apex development in spring wheat. *Agron. J.*, **74**, 504-509.

Frank, A.B., Bauer, A. and Black, A.L. (1987) Effects of air-temperature and water-stress on apex development in spring wheat. *Crop Sci.*, **27**, 113-116.

Glenn, P., Woods, D.P., Zhang, J., Gabay, G., Odle, N. and Dubcovsky, J. (2023) Wheat bZIPC1 interacts with FT2 and contributes to the regulation of spikelet number per spike. *Theor. Appl. Genet.*, **136**, 237.

Glenn, P., Zhang, J., Brown-Guedira, G., DeWitt, N., Cook, J.P., Li, K., Akhunov, E. and Dubcovsky, J. (2022) Identification and characterization of a natural polymorphism in *FT-A2* associated with increased number of grains per spike in wheat. *Theor Appl Genet*, **135**, 679-692.

Goslin, K., Zheng, B.B., Serrano-Mislata, A., Rae, L., Ryan, P.T., Kwasniewska, K., Thomson, B., O'Maoiléidigh, D.S., Madueño, F., Wellmer, F. and Graciet, E. (2017) Transcription factor interplay between LEAFY and APETALA1/CAULIFLOWER during floral initiation. *Plant Physiol.*, **174**, 1097-1109.

Huala, E. and Sussex, I.M. (1992) Leafy interacts with floral homeotic genes to regulate Arabidopsis floral development. *Plant Cell*, **4**, 901-913.

Ikeda-Kawakatsu, K., Maekawa, M., Izawa, T., Itoh, J.I. and Nagato, Y. (2012) *ABERRANT PANICLE ORGANIZATION 2/RFL*, the rice ortholog of Arabidopsis *LEAFY*, suppresses the transition from inflorescence meristem to floral meristem through interaction with *APO1*. *Plant J.*, **69**, 168-180.

Ikeda, K., Ito, M., NagasawaO, N., Kyozuka, J. and Nagato, Y. (2007) Rice *ABERRANT PANICLE ORGANIZATION 1*, encoding an F-box protein, regulates meristem fate. *Plant J.*, **51**, 1030-1040.

Ikeda, K., Nagasawa, N. and Nagato, Y. (2005) *ABERRANT PANICLE ORGANIZATION 1* temporally regulates meristem identity in rice. *Dev. Biol.*, **282**, 349-360.

Jin, R., Klasfeld, S., Zhu, Y., Garcia, M.F., Xiao, J., Han, S.K., Konkol, A. and Wagner, D. (2021) LEAFY is a pioneer transcription factor and licenses cell reprogramming to floral fate. *Nat. Commun.*, **12**.

Kaufmann, K., Wellmer, F., Muino, J.M., Ferrier, T., Wuest, S.E., Kumar, V., Serrano-Mislata, A., Madueno, F., Krajewski, P., Meyerowitz, E.M., Angenent, G.C. and Riechmann, J.L. (2010) Orchestration of floral initiation by APETALA1. *Science*, **328**, 85-89.

Krasileva, K.V., Vasquez-Gross, H.A., Howell, T., Bailey, P., Paraiso, F., Clissold, L., Simmonds, J., Ramirez-Gonzalez, R.H., Wang, X., Borrill, P., Fosker, C., Ayling, S., Phillips, A.L., Uauy, C. and Dubcovsky, J. (2017) Uncovering hidden variation in polyploid wheat. *Proc. Natl. Acad. Sci. USA*, **114**, E913-E921.

Kuzay, S., Lin, H., Li, C., Chen, S., Woods, D., Zhang, J. and Dubcovsky, J. (2022) *WAPO-A1* is the causal gene of the 7AL QTL for spikelet number per spike in wheat. *PLoS Genet.*, **18**, e1009747.

Kuzay, S., Xu, Y., Zhang, J., Katz, A., Pearce, S., Su, Z., Fraser, M., Anderson, J.A., Brown-Guedira, G., DeWitt, N., Peters Haugrud, A., Faris, J.D., Akhunov, E., Bai, G. and Dubcovsky, J. (2019) Identification of a candidate gene for a QTL for spikelet number per spike on wheat chromosome arm 7AL by high-resolution genetic mapping. *Theor Appl Genet*, **132**, 2689–2705.

Kyozuka, J., Konishi, S., Nemoto, K., Izawa, T. and Shimamoto, K. (1998) Down-regulation of *RFL*, the *FLO/LFY* homolog of rice, accompanied with panicle branch initiation. *Proc. Natl. Acad. Sci. USA*, **95**, 1979-1982.

Lee, I., Wolfe, D.S., Nilsson, O. and Weigel, D. (1997) A *LEAFY* co-regulator encoded by *UNUSUAL FLORAL ORGANS*. *Curr. Biol.*, **7**, 95-104.

Levin, J.Z. and Meyerowitz, E.M. (1995) *Ufo* - an Arabidopsis gene involved in both floral meristem and floral organ development. *Plant Cell*, **7**, 529-548.

Li, C. and Dubcovsky, J. (2008) Wheat FT protein regulates *VRN1* transcription through interactions with FDL2. *Plant J.*, **55**, 543-554.

Li, C., Lin, H., Chen, A., Lau, M., Jernstedt, J. and Dubcovsky, J. (2019) Wheat *VRN1*, *FUL2* and *FUL3* play critical and redundant roles in spikelet development and spike determinacy. *Development*, **146**, dev175398.

Li, C., Lin, H. and Dubcovsky, J. (2015) Factorial combinations of protein interactions generate a multiplicity of florigen activation complexes in wheat and barley. *Plant J.*, **84**, 70-82.

Liu, Y.Y., Chen, J., Yin, C.B., Wang, Z.Y., Wu, H., Shen, K.C., Zhang, Z.L., Kang, L.P., Xu, S., Bi, A.Y., Zhao, X.B., Xu, D.X., He, Z.H., Zhang, X.Y., Hao, C.Y., Wu, J.H., Gong, Y., Yu, X.C., Sun, Z.W., Ye, B.T., Liu, D.N., Zhang, L.L., Shen, L.P., Hao, Y.F., Ma, Y.Z., Lu, F. and Guo, Z.F. (2023) A high-resolution genotype-phenotype map identifies the controlling grain number and size in wheat. *Genome Biol.*, **24**.

Lv, B., Nitcher, R., Han, X., Wang, S., Ni, F., Li, K., Pearce, S., Wu, J., Dubcovsky, J. and Fu, D. (2014) Characterization of *FLOWERING LOCUS T1* (*FT1*) gene in *Brachypodium* and wheat. *PLoS One*, **9**, e94171.

Maas, E.V. and Grieve, C.M. (1990) Spike and leaf development in salt-stressed wheat. *Crop Sci.*, **30**, 1309-1313.

Maccaferri, M., Harris, N.S., Twardziok, S.O., Pasam, R.K., Gundlach, H., Spannagl, M., Ormanbekova, D., Lux, T., Prade, V.M., Milner, S.G., Himmelbach, A., Mascher, M., Bagnaresi, P., Faccioli, P., Cozzi, P., Lauria, M., Lazzari, B., Stella, A., Manconi, A., Gnocchi, M., Moscatelli, M., Avni, R., Deek, J., Biyiklioglu, S., Frascaroli, E., Corneti, S., Salvi, S., Sonnante, G., Desiderio, F., Mare, C., Crosatti, C., Mica, E., Ozkan, H., Kilian, B., De Vita, P., Marone, D., Joukhadar, R., Mazzucotelli, E., Nigro, D., Gadaleta, A., Chao, S.M., Faris, J.D., Melo, A.T.O., Pumphrey, M., Pecchioni, N., Milanesi, L., Wiebe, K., Ens, J., MacLachlan, R.P., Clarke, J.M., Sharpe, A.G., Koh, C.S., Liang, K.Y.H., Taylor, G.J., Knox, R., Budak, H., Mastrangelo, A.M., Xu, S.S., Stein, N., Hale, I., Distelfeld, A., Hayden, M.J., Tuberosa, R., Walkowiak, S., Mayer, K.F.X., Ceriotti, A., Pozniak, C.J. and Cattivelli, L. (2019) Durum wheat genome highlights past domestication signatures and future improvement targets. *Nat. Genet.*, **51**, 885-895.

Miao, Y.L., Xun, Q., Taji, T., Tanaka, K., Yasuno, N., Ding, C.Q. and Kyozuka, J. (2022) *ABERRANT PANICLE ORGANIZATION2* controls multiple steps in panicle formation through common direct-target genes. *Plant Physiol.*, **189**, 2210-2226.

Molinero-Rosales, N., Jamilena, M., Zurita, S., Gómez, P., Capel, J. and Lozano, R. (1999) *FALSIFLORA*, the tomato orthologue of *FLORICAULA* and *LEAFY*, controls flowering time and floral meristem identity. *Plant J.*, **20**, 685-693.

Pajoro, A., Madrigal, P., Muino, J.M., Matus, J.T., Jin, J., Mecchia, M.A., Debernardi, J.M., Palatnik, J.F., Balazadeh, S., Arif, M., O'Maoileidigh, D.S., Wellmer, F., Krajewski, P., Riechmann, J.L., Angenent, G.C. and Kaufmann, K. (2014) Dynamics of chromatin accessibility and gene regulation by MADS-domain transcription factors in flower development. *Genome Biol.*, **15**.

Preston, J.C., Christensen, A., Malcomber, S.T. and Kellogg, E.A. (2009) MADS-box gene expression and implications for developmental origins of the grass spikelet. *Amer. Jour. Bot.*, **96**, 1419-1429.

Ream, T.S., Woods, D.P., Schwartz, C.J., Sanabria, C.P., Mahoy, J.A., Walters, E.M., Kaeppler, H.F. and Amasino, R.M. (2014) Interaction of photoperiod and vernalization determines flowering time of *Brachypodium distachyon*. *Plant Physiol.*, **164**, 694-709.

Rieu, P., Turchi, L., Thevenon, E., Zarkadas, E., Nanao, M., Chahtane, H., Tichtinsky, G., Lucas, J., Blanc-Mathieu, R., Zubieta, C., Schoehn, G. and Parcy, F. (2023) The F-box protein UFO controls flower development by redirecting the master transcription factor LEAFY to new cis-elements. *Nat. Plants*, **9**, 315-+.

Sato, K., Abe, F., Mascher, M., Haberer, G., Gundlach, H., Spannagl, M., Shirasawa, K. and Isobe, S. (2021) Chromosome-scale genome assembly of the transformation-amenable common wheat cultivar 'Fielder'. *DNA Res*, **28**, dsab008.

Schultz, E.A. and Haughn, G.W. (1991) *LEAFY*, a homeotic gene that regulates inflorescence development in Arabidopsis. *Plant Cell*, **3**, 771-781.

Selva, C., Shirley, N.J., Houston, K., Whitford, R., Baumann, U., Li, G. and Tucker, M.R. (2021) *HvLEAFY* controls the early stages of floral organ specification and inhibits the formation of multiple ovaries in barley. *Plant J.*, **108**, 509-527.

Shaw, L.M., Lyu, B., Turner, R., Li, C., Chen, F., Han, X., Fu, D. and Dubcovsky, J. (2019) *FLOWERING LOCUS T2* regulates spike development and fertility in temperate cereals. *J. Exp. Bot.*, **70**, 193–204.

Shaw, L.M., Turner, A.S., Herry, L., Griffiths, S. and Laurie, D.A. (2013) Mutant alleles of *Photoperiod-1* in wheat (*Triticum aestivum* L.) that confer a late flowering phenotype in long days. *PLoS One*, **8**, e79459.

Shitsukawa, N., Takagishi, A., Ikari, C., Takumi, S. and Murai, K. (2006) WFL, a wheat FLORICAULA/LEAFY ortholog, is associated with spikelet formation as lateral branch of the inflorescence meristem. *Genes & Genetic Systems*, **81**, 13-20.

Souer, E., van der Krol, A., Kloos, D., Spelt, C., Bliek, M., Mol, J. and Koes, R. (1998) Genetic control of branching pattern and floral identity during inflorescence development. *Development*, **125**, 733-742.

VanGessel, C., Hamilton, J., Tabbita, F., Dubcovsky, J. and Pearce, S. (2022) Transcriptional signatures of wheat inflorescence development. *Sci Rep-Uk*, **12**, 17224.

Wagner, D., Sablowski, R.W.M. and Meyerowitz, E.M. (1999) Transcriptional activation of *APETALA1* by LEAFY. *Science*, **285**, 582-584.

Walkowiak, S., Gao, L.L., Monat, C., Haberer, G., Kassa, M.T., Brinton, J., Ramirez-Gonzalez, R.H., Kolodziej, M.C., Delorean, E., Thambugala, D., Klymiuk, V., Byrns, B., Gundlach, H., Bandi, V., Siri, J.N., Nilsen, K., Aquino, C., Himmelbach, A., Copetti, D., Ban, T., Venturini, L., Bevan, M., Clavijo, B., Koo, D.H., Ens, J., Wiebe, K., N'Diaye, A., Fritz, A.K., Gutwin, C., Fiebig, A., Fosker, C., Fu, B.X., Accinelli, G.G., Gardner, K.A., Fradgley, N., Gutierrez-Gonzalez, J., Halstead-Nussloch, G., Hatakeyama, M., Koh, C.S., Deek, J., Costamagna, A.C., Fobert, P., Heavens, D., Kanamori, H., Kawaura, K., Kobayashi, F., Krasileva, K., Kuo, T., McKenzie, N., Murata, K., Nabeka, Y., Paape, T., Padmarasu, S., Percival-Alwyn, L., Kagale, S., Scholz, U., Sese, J., Juliana, P., Singh, R., Shimizu-Inatsugi, R., Swarbreck, D., Cockram, J., Budak, H., Tameshige, T., Tanaka, T., Tsuji, H., Wright, J., Wu, J.Z., Steuernagel, B., Small, I., Cloutier, S., Keeble-Gagnere, G., Muehlbauer, G., Tibbets, J., Nasuda, S., Melonek, J., Hucl, P.J., Sharpe, A.G., Clark, M., Legg, E., Bharti, A., Langridge, P., Hall, A., Uauy, C., Mascher, M., Krattinger, S.G., Handa, H., Shimizu, K.K., Distelfeld, A., Chalmers, K., Keller, B., Mayer, K.F.X., Poland, J., Stein, N., McCartney, C.A., Spannagl, M., Wicker, T. and Pozniak, C.J. (2020) Multiple wheat genomes reveal global variation in modern breeding. *Nature*, **588**, 277-283.

Weigel, D., Alvarez, J., Smyth, D.R., Yanofsky, M.F. and Meyerowitz, E.M. (1992) Leafy controls floral meristem identity in Arabidopsis. *Cell*, **69**, 843-859.

Weigel, D. and Nilsson, O. (1995) A developmental switch sufficient for flower Initiation in diverse plants. *Nature*, **377**, 495-500.

Wilkinson, M.D. and Haughn, G.W. (1995) *UNUSUAL FLORAL ORGANS* controls meristem identity and organ primordia fate in Arabidopsis. *Plant Cell*, **7**, 1485-1499.

William, D.A., Su, Y.H., Smith, M.R., Lu, M., Baldwin, D.A. and Wagner, D. (2004) Genomic identification of direct target genes of LEAFY. *Proc. Natl. Acad. Sci. USA*, **101**, 1775-1780.

Winter, C.M., Yamaguchi, N., Wu, M.F. and Wagner, D. (2015) Transcriptional programs regulated by both LEAFY and APETALA1 at the time of flower formation. *Physiol. Plantarum*, **155**, 55-73.

Yan, L., Loukoianov, A., Tranquilli, G., Helguera, M., Fahima, T. and Dubcovsky, J. (2003) Positional cloning of wheat vernalization gene *VRN1*. *Proc. Natl. Acad. Sci. USA*, **100**, 6263-6268.

Yoshida, H. (2012) Is the lodicule a petal: Molecular evidence? *Plant Sci.*, **184**, 121-128.

Zhang, J., Li, C., Zhang, W., Zhang, X., Mo, Y., Tranquilli, G.E., Vanzetti, L.S. and Dubcovsky, J. (2023a) Wheat plant height locus *RHT25* encodes a PLATZ transcription factor that interacts with DELLA (RHT1). *Proc. Natl. Acad. Sci. USA*, **120**, e2300203120.

Zhang, J., Xiong, H., Burguener, G.F., Vasquez-Gross, H., Liu, Q., Debernardi, J.M., Akhunova, A., Garland-Campbell, K., Kianian, S.F., Brown-Guedira, G., Pozniak, C., Faris, J.D., Akhunov, E. and Dubcovsky, J. (2023b) Sequencing 4.3 million mutations in wheat promoters to understand and modify gene expression. *Proc. Natl. Acad. Sci. USA*, **120**, e2306494120.

Zhang, J.L., Gizaw, S.A., Bossolini, E., Hegarty, J., Howell, T., Carter, A.H., Akhunov, E. and Dubcovsky, J. (2018) Identification and validation of QTL for grain yield and plant water status under contrasting water treatments in fall-sown spring wheats. *Theor. Appl. Genet.*, **131**, 1741-1759.

Zhong, J., van Esse, G.W., Bi, X., Lan, T., Walla, A., Sang, Q., Franzen, R. and von Korff, M. (2021) *INTERMEDIUM-M* encodes an HvAP2L-H5 ortholog and is required for inflorescence indeterminacy and spikelet determinacy in barley. *P Natl Acad Sci USA*, **118**, e2011779118.